Full Paper

Title:

Metal toxicity contributes to the structuring of bacterial communities in the Arabidopsis phyllosphere

Author names and affiliations:

Jan F. Plewka-Mandelkow[1], Anna S. Thomas[1], Julia A. Vorholt[2], Ute Krämer[1§]

[1]Faculty of Biology and Biotechnology, Ruhr University Bochum, 44801 Bochum, Germany

[2]Institute of Microbiology, ETH Zurich, Zurich, Switzerland

[§]**Corresponding author**:

Professor Dr. Ute Krämer
Molecular Genetics and Physiology of Plants
Ruhr University Bochum
Universitätsstraße 150, Box 44, ND3/30
D-44801 Bochum, Germany
Tel.: +49 (0)234 32 24291, FAX: +49 (0)234 32 14187
Email: Ute.Kraemer@ruhr-uni-bochum.de

ORCID: 0009-0005-9889-7593 (JFP-M), 0000-0002-6011-4910 (JV), 0000-0001-7870-4508 (UK)

Word counts: Introduction (974), Materials and Methods (979), Results (3,081), Discussion (2,546), Total: 7,580. 7 Figures (colored), 1 Table, Supporting Information (7 Figures, 10 Tables, 7 Datasets).

Summary

- The causal factors shaping plant-associated microbiota are incompletely known. Elevated concentrations of the micronutrients zinc (Zn), manganese (Mn) and copper (Cu), and exposure to non-essential trace elements including cadmium (Cd) and arsenic (As), can be toxic. Here we explored whether differences in metal(loid) sensitivity between plants and bacteria influence phyllosphere bacterial community composition.
- 224 representative *Arabidopsis thaliana* phyllosphere bacterial strains were screened on metal(loid) concentration series in synthetic media. We obtained leaf apoplastic fluid ionomes for comparisons with bacteriotoxicity profiles, and tested for relationships between strain-wise metal(loid) tolerances, phylogeny and gene content.
- Leaf apoplastic Zn^{2+} and Cd^{2+} concentrations were the most likely to arrest growth of metal-sensitive bacteria *in planta*. Soil bacterial strains were several-fold more sensitive to both these metals than leaf strains, consistent with selection for increased bacterial Zn and Cd tolerance in the phyllosphere. Strains known to govern bacterial community structure were metal-sensitive, with only minor influences of between-metal and between-strain interactions. Bacterial genus explained considerable proportions of the variances in metal(loid)-related gene content and tolerance phenotypes. Bacterial Cd tolerance correlated with the presence and copy number of known Cd-related genes.
- Our results suggest that plant metal homeostasis contributes to structuring bacterial communities in the leaf endosphere.

Keywords

Arabidopsis thaliana, leaf apoplast, phyllosphere, endosphere, synthetic communities, cadmium, zinc, microbiota

54 ## Introduction

55 Diversity among bacteria is unparalleled, and they have colonized the broadest range of habitats
56 in the world, including soil, water, and multicellular organisms. The plant-associated microbiota
57 comprises complex microbial communities influenced by the plant host, microbe-microbe
58 interactions, and other environmental factors, and they can have positive effects on plant fitness
59 (Müller *et al.*, 2016b; Ritpitakphong *et al.*, 2016; Vogel *et al.*, 2021). The phyllosphere is one of
60 the largest habitats for bacteria with an estimated global area of around 1 billion km^2 (Vorholt,
61 2012) and comprises two distinct microbial habitats: one on the outer leaf surfaces named the
62 phylloplane, and one inside the leaf named the endosphere. The leaf endosphere is accessible from
63 the leaf surface *via* the stomata while they are open. Within a given plant organ, the volume outside
64 the plasma membranes bordering all cells is referred to as the apoplast, comprising both the cell
65 walls and the intercellular space in between (Sattelmacher, 2001). In general, the leaf apoplast is
66 at least partially filled with an extracellular solution, and the remainder of it is occupied by air. In
67 addition to its role as a habitat for endosphere microbial communities, the apoplast serves as a site
68 for the inter-cellular movement of gases, water and solutes, as well as for the storage and
69 detoxification of organic and inorganic compounds including metals (Küpper *et al.*, 2000;
70 Sattelmacher, 2001; Kajala *et al.*, 2019).

71 Impacts on bacteria inhabiting the phylloplane, rhizosphere and rhizoplane are determined
72 predominantly by the environment around the plant. The closer the plant host, the stronger is its
73 influence on the microbiota (Bulgarelli *et al.*, 2013; Chen *et al.*, 2020). The plant begins to exert
74 some control over the composition of its apoplast progressively from the root epidermis inwards,
75 where both diffusion from the soil solution and microbial colonization can occur easily on the
76 external side of apoplastic barriers, or during root developmental stages prior to their formation.
77 In roots, apoplastic barriers are constituted by the Casparian strip that is positioned radially around
78 root endodermal cells as well as the suberization of the outwardly oriented surfaces of epidermal
79 and endodermal cell layers, both initiated at specific stages of differentiation. Endodermal
80 suberization is plastic to some degree and regulated dependent on both the plant's nutritional status
81 and plant-associated microbial communities (Robb *et al.*, 1991; Andersen *et al.*, 2015; Barberon
82 *et al.*, 2016). The apoplast on the internal side of the root apoplastic barriers and of the leaf
83 endosphere represent comparably sheltered niches for the inhabiting microbes. At these sites, the

84 plant host has a predominant influence on apoplast composition, thus providing opportunities for
85 niche construction by the plant. To date, little is known about the composition of this micro-habitat
86 and any evolutionary adaptations to it in the inhabiting microbes.

87 The plant apoplast is known to function in the storage and detoxification of excess metal cations,
88 including those of so-called heavy metals, or – more accurately – class B (e.g., Cu^{+}) and borderline
89 elements (e.g., Cu^{2+}, Cd^{2+}, Fe^{2+}, Fe^{3+}, Mn^{2+}, Zn^{2+} (Nieboer, 1980; Farvardin *et al.*, 2020)). Among
90 these, the micronutrients (mostly Fe, Zn, Cu, Mn and Ni) are required in small quantities by all
91 organisms to serve as or within protein cofactors acting in ligand binding and in the catalysis of a
92 variety of chemical reactions (Pais & Jones, 1997; Marschner & Marschner, 2012). Because of
93 their powerful chemical properties, these same nutrients can become highly toxic even when
94 present in slight excess. Moreover, chemically similar non-essential trace elements are
95 ubiquitously present in the environment, for example Cd. All organisms, including bacteria and
96 plants, possess metal homeostasis networks which operate to fulfill nutritional requirements while
97 counteracting metal toxicities across their specific environmental ranges (Clemens, 2001; Nies &
98 Grass, 2009; Chandrangsu *et al.*, 2017). Over the course of evolution, metal homeostasis networks,
99 as well as nutritional metal needs, have diverged between bacteria, fungi and plants to some extent.
100 For example, the metalloproteome of plants generally requires more Cu and Zn, and less Ni, than
101 that of most bacteria (Williams, 2007). This divergence implies that metal concentrations
102 maintained and tolerated by the plant within the apoplast may be inhibitory to bacterial colonists,
103 raising the possibility that plants modulate apoplastic metal levels to selectively influence
104 microbial community composition. In support of this, *Arabidopsis thaliana* Zn^{2+} efflux ATPases
105 HMA2 and HMA4 are required for resistance to the necrotrophic fungal pathogen
106 *Plectosphaerella cucumerina* (Escudero *et al.*, 2022), for example, demonstrating that plant-
107 controlled apoplastic metal levels can shape interactions with invading microbes. Moreover, high
108 leaf apoplastic zinc concentrations can directly protect the metal hyperaccumulator *Noccaea*
109 *caerulescens* (ecotype Prayon) against infection by *Pseudomonas syringae* pv. maulicola M4
110 (Fones *et al.*, 2010). The concept of nutritional immunity is well-established through medical
111 research, whereby the host manipulates nutrient availability to limit pathogen growth. However,
112 related concepts are less well understood and remain underexplored in plant science (Fones &
113 Preston, 2013; Murdoch & Skaar, 2022; Krämer, 2024).

114 Here we explored the relationship between metal(loid) levels in the plant apoplast and plant-
115 associated microbial communities. We profiled the metal(loid) tolerances of 224 representative
116 phyllosphere bacterial strains of the *At*-LSPHERE collection, a curated set of isolates from the
117 model plant *A. thaliana* (Bai *et al.*, 2015), focusing on elements that could reach bacteriotoxic
118 levels inside leaves of plants in their natural non-contaminated environments: Cd, Cu, Mn, Zn, and
119 arsenic. We then generated ionomic data for the Arabidopsis leaf apoplast, which we evaluated in
120 the context of phyllosphere bacterial metal(loid) tolerances as well as in comparison to tolerance
121 profiles of soil bacteria, and we identified genomic predictors of metal tolerance in phyllosphere
122 bacterial strains. Combining these datasets, we assessed whether metal(loid) co-tolerance patterns
123 reflect shared chemical properties or environmental selection. In summary, our work identifies the
124 modulation of Zn and Cd levels in the leaf apoplast as a potential means for plants to shape the
125 bacterial community in the leaf endosphere.

126

127 ## Materials and Methods

128 **Biological materials and cultivation conditions**

129 *Arabidopsis thaliana* (L.) Heynh., accession Columbia (Col-0), wild-type seeds (Lehle Seeds,
130 Round Rock, TX, USA) were sown onto moistened standard soil (Type Minitray, Balster
131 Einheitserdewerk, Fröndenberg, Germany) and stratified in darkness at 4°C for 2 d, followed by
132 cultivation in 8-h light (145 µmol m^{-2} s^{-1}, 22°C)/16-h dark (18°C) cycles in a growth chamber
133 (GroBank BB-XXL.3, CLF Plant Climatics, Wertingen, Germany). After 2 w, single seedlings
134 were transferred into 0.7-L pots containing standard soil or a mix of a natural soil from Bad
135 Gottleuba, 50°50'45.7" N 13°59'43.1" E, with sand and standard soil (35 + 15 + 50 volume parts,
136 respectively), and cultivated for another 5 to 6 w.

137 The 224 isolates of the *A. thaliana* phyllosphere (*At*-LSPHERE; Bai et al. 2015) collection and the
138 33 bacterial isolates from unplanted soil (Bai *et al.*, 2015) were cultivated in 3 mL liquid R2A
139 medium containing methanol (0.5% v/v) in darkness at RT, with continuous shaking (300 rpm),
140 for 2 to 3 d. Saturated cultures were mixed 1:1 (v:v) with sterile-filtered 70% (v/v) glycerol in
141 ultrapure water and stored at -80°C. All cultivation was conducted in R2A media containing
142 methanol (0.5% v/v), prepared and autoclaved as described (Bai *et al.*, 2015), and subsequently

143 supplemented with metal(loid)s from sterile-filtered (Filtropur S 0.2 µm, SARSTEDT AG & Co.
144 KG, Nürmbrecht, Germany) stock solutions where needed (Tables S1 and S2).

145 **High-throughput metal(loid) tolerance screening**

146 Bacterial stocks were defrosted and screened on agar-solidified media in square polystyrene petri
147 plates (120 x 120 x 17 mm) using a sterilized 96-pin microplate replicator (Boekel Scientific,
148 Feasterville, USA), followed by incubation at RT in the dark. Growth was scored based on
149 photographs taken after 10 d and 20 d (occasionally) of cultivation. Three independent experiments
150 (repeats) were conducted, each comprising a control of unamended medium and a series of six
151 concentrations for each metal(loid) (Table S2). Additional metal(loid) concentrations were tested
152 in further experiments.

153 **Quantification of Metal(loid) Tolerances in Single Strains and Synthetic Communities**

154 Single colonies of keystone strains (Carlström *et al.*, 2019) and of each strains of the synthetic
155 communities (SynComs) were transferred into 3 mL of liquid medium and pre-cultivated at RT
156 for 1 to 2 d. Each culture was diluted with sterile liquid medium to an OD_{600} of 0.2 (SYNERGY
157 HTX multi-mode reader, BioTek Instruments GmbH, Bad Friedrichshall, Germany), mixed 1:1
158 (v:v) with 70% (v/v) sterile-filtered glycerol, with equal volumes used per strain to assemble each
159 of the SynComs, and stored at -80°C. For the quantification of metal tolerances based on growth
160 curves, five µL of each stock were added per well containing 195 µL liquid medium with or
161 without (control) metal supplementation in a 96-well plate. Bacterial strains were cultivated in
162 darkness at 22 to 28°C for ≥ 20 h (Cd tolerance) and 48 h (combined metal toxicities), with one
163 OD_{600} measurement per h (5 technical replicates per experiment, 3 independent experiments) or
164 per 0.5 h (SynComs; 6 technical replicates per experiment, 5 independent experiments) preceded
165 by horizontal shaking at 200 rpm for 5 min.

166 **Isolation of leaf apoplastic wash fluid from *A. thaliana* and Multi-Element Analyses**

167 Apoplastic wash fluid was prepared as described (O'Leary *et al.*, 2014), with small modifications.
168 Freshly harvested leaves were immersed in an infiltration fluid (IF) of either ultrapure water or
169 100 µM EDTA (pH 7.2), followed by three cycles of vacuum-infiltration at 30 mbar for 3 min and
170 release of the vacuum over a period of 3 min, with recovery of the AWF by centrifugation in a
171 swinging bucket rotor at 1,000x*g* and 4°C for 15 min. We experimentally determined a dilution

172 factor for the AF in the AWF (2.35; $n = 4$) (O'Leary *et al.*, 2014). For multi-element analyses, dry
173 aliquots of AWF, leaf powder, liquid media, agar and soils were acid-digested, followed by
174 Inductively Coupled Plasma-Optical Emission Spectrometry (ICP-OES) using an iCAP Duo 6500
175 (Thermo Fisher, Dreieich, Germany) (Stein *et al.*, 2017) (see also Supporting Methods).

176 **Data Analyses and Visualization**

177 Data were organized in Microsoft Excel (Microsoft Corporation, Redmond, USA), with analysis
178 using R (version 4.3.0) (R_Core_Team, 2020) in the RStudio environment (version
179 2023.06.0.421) (RStudio_Team, 2021) and plot post-processing in Inkscape (version 1.2.2)
180 (Inkscape_Project, 2020). Dose-response curves ($f(x) = E_{inf}+(1-E_{inf})/(1+(x/EC_{50})^h)$) and metrics
181 ($EC_n = EC_{50} \times [(0.01\ n)/(1 - 0.01\ n - E_{inf})]^{1/h}$) were obtained using the `GRfit()` function of the
182 *GRmetrics* package (E_{inf} : proportion of bacteria surviving an infinite metal concentration, set to 0
183 for calculating EC_n; EC_n: metal(loid) concentration at which n% of the strains were unable to grow;
184 h: Hill coefficient of the fitted curve; x the metal concentration in the medium [mM]; and $f(x)$ the
185 proportion of surviving strains). We calculated strain-wise MPC for each metal(loid) as the median
186 of three independent experiments, followed by conversion to z-scores across all strains for each
187 metal(loid) using `scale()`. A Euclidean distance matrix for hierarchical clustering was
188 generated with the `dist()` function. Based on an agglomerative coefficient of 0.98 calculated
189 using the `agnes()` of *cluster*, Ward clustering was the best-fitting method and implemented
190 through `hclust()` using the ward.D2 method. Principal component analyses (PCAs) were
191 conducted using `prcomp()`, with significance testing using *PCAtest*. Null distributions for PCA
192 statistics were generated using 999 random permutations, and sampling variance was estimated
193 based on 999 bootstrap replicates. The `capscale()` function of *vegan* was used for constrained
194 principal coordinate analyses (CPCoA). Statistical significance of the ordinations and confidence
195 intervals for the variance were calculated by ANOVA-like permutation tests using
196 `permutest()` and `anova.cca()` (Robbins *et al.*, 2018). We calculated growth rate $r = ln(OD_{600}(T_2)/OD_{600}(T_1))/(T_2-T_1)$ and apparent doubling time $t_d = \ln(2)/r$ from the first Log phase
198 of growth between Time points T_1 and T_2 identified using the *zoo* package and a linear model (ln-
199 transformed OD_{600}). The phylogenetic tree was built with `bionj()` from *ape* using 16s rRNA
200 sequences (Bai *et al.*, 2015) (www.at-sphere.com) aligned with `msa()` followed by the

201 computation of a distance matrix using `msaConvert()` from *msa* and `dist.alignment()`
202 from *seqinr*.

203

204 Results

205 Profiles of metal(loid) tolerances among Arabidopsis phyllosphere bacterial strains

206 To obtain insights into whether the metal(loid) levels in the leaf apoplast can influence the
207 composition of phyllosphere microbial communities, we profiled the tolerance limits of all
208 individual strains within the publicly available representative collection of Arabidopsis leaf
209 phyllosphere bacteria named *At*-LSPHERE (n = 224) (Bai *et al.*, 2015). For comparison, we
210 additionally screened a collection of bacteria from unplanted soil (n = 33) (Bai *et al.*, 2015) in the
211 same manner. We spotted bacterial suspensions of each strain on agar-solidified R2A media
212 supplemented with concentration series of the essential metals copper (Cu^{II}), zinc (Zn^{II}), and
213 manganese (Mn^{II}), as well as of the non-essential trace metal cadmium (Cd^{II}), and the metalloid
214 arsenic (As) in two common inorganic forms, arsenite (As^{III}) and arsenate (As^{V}) (Tables S1 to S3).

215 Of all tested metal(loid)s, Cd^{II} was toxic for some *At*-LSPHERE strains at the lowest concentration
216 (0.8 µM; Dataset S1). A concentration of 49 µM Cd eliminated the growth of 50% of the bacterial
217 strains (termed here Effective Concentration EC_{50}), with a factor of 130 between the Cd
218 concentrations eliminating the 5% most sensitive (EC_5) and the 5% most tolerant strains (EC_{95}),
219 defined here as concentration range (Fig. 1a, Table 1). Compared to phyllosphere bacterial strains,
220 soil bacteria were more sensitive to Cd, with EC_5, EC_{50} and EC_{95} concentrations of approximately
221 50%, 20% and 10%, respectively, and only about one-fifth of the concentration range (Fig. 1b,
222 Table 1).

223 We observed EC_{50} values of 0.42, 0.5, and 1.1 mM, respectively, for the trace elements Cu^{II}, Zn^{II},
224 and arsenite. Of these three elements, Zn began to impede the growth of some phyllosphere
225 bacterial strains at the lowest concentration (EC_5 of 46 µM), and it continued to permit the growth
226 of the most tolerant strains up to the highest concentration (10 mM; Dataset S1, Fig. 1a, Table 1),
227 with a concentration range of 120, very similar to that for Cd. Soil bacteria were less Zn-tolerant,
228 showing EC_5, EC_{50} and EC_{95} concentrations of approximately 90%, 30% and 12%, respectively,

229 and only about one-seventh of the concentration range, compared to phyllosphere bacteria (Fig.
230 1b, Table 1).

231 The 15-fold difference in Cu concentration between the EC_5 of 0.11 and the EC_{95} of 1.6 mM was
232 the narrowest among all metal(loid)s tested in phyllosphere bacteria. Compared to phyllosphere
233 bacteria, soil bacteria were more Cu-tolerant, with approximately 2-fold EC_5, 1.5-fold EC_{50}, and a
234 similar EC_{95}, despite a narrower concentration range of approximately one-third of that observed
235 in phyllosphere bacteria. Arsenite was less toxic to phyllosphere bacteria than Cd^{II}, Cu^{II}, and Zn^{II},
236 with an EC_{50} of 1.1 mM (Fig. 1a, Table 1).

237 The EC_{50} of Mn^{II} was as high as 9.2 mM, and arsenate was the least harmful to *At*-LSPHERE
238 strains. At the highest tested arsenate concentration of 100 mM, about 50% of the bacterial strains
239 were still able to grow, although we depleted phosphate in these media (Tables S1 to S3). For As
240 and Mn, phyllosphere bacteria tended to have higher EC_5 concentrations than soil bacteria (about
241 2-fold for As^{III} and 4-fold for Mn^{II}), similar EC_{50} concentrations, and lower EC_{95} concentrations,
242 clearly different from Zn, Cd and Cu (Fig. 1a and b, Table 1). Taken together, these results
243 suggested that bacterial strains with elevated Cd^{II} and Zn^{II} tolerance are enriched in the
244 phyllosphere of Arabidopsis compared to unplanted soil under natural field conditions.

245 We next investigated whether the metal tolerances of single strains are representative of those of
246 bacterial communities, using Cd tolerance as an example. We designed three synthetic
247 communities (SynComs) comprising strains that individually exhibited high, intermediate and low
248 Cd tolerance, respectively (Table S4). The composition of these SynComs matched the
249 phylogenetic profile of phyllosphere communities as closely as possible (Fig. S1). On solid R2A
250 media, growth of the SynComs reflected that of the most tolerant strain in single-strain assays (Fig.
251 S2a and S2b). In liquid R2A media, the relative Cd tolerances of SynComs also qualitatively
252 followed those observed for single strains on solid media, but Cd toxicity was more severe in liquid
253 media (Figs. 1c and S3, compare with Fig. S2 and Table 1). These results supported the relevance
254 of our single-strain tolerance assays for exemplary bacterial communities.

255 **The magnitudes of apoplastic Cd and Zn concentrations reach levels toxic to a subset of**
256 **phyllosphere bacterial strains**

257 To assess whether phyllosphere bacteria might encounter toxic metal levels in the leaf endosphere,
258 we analyzed the composition of the leaf apoplastic fluid (AF). We cultivated *A. thaliana* in

259 standard greenhouse soil or in a field-collected soil from a region known for geogenically slightly
260 elevated total Cd levels (Stein *et al.*, 2017) for 7 to 8 weeks, and extracted apoplastic wash fluid
261 (AWF) using the infiltration-centrifugation technique (Tables S5 and S6) (O'Leary *et al.*, 2014;
262 Figueiredo *et al.*, 2021). AWF is commonly obtained using water as an infiltration fluid (IF). The
263 IF might affect metal solubility during the experimental procedure, for instance by increasing the
264 extracellular pH within infiltrated leaves. Therefore, we interpret the corresponding results as
265 estimates of the minimal metal levels encountered in the AF. Cell walls contain bound metal
266 cations, which continuously equilibrate with the surrounding AF and can thus be taken up by
267 microbes. To obtain estimates of the maximal metal concentrations in the AF, we used as the IF a
268 solution of 100 µM ethylenediaminetetraacetic acid (EDTA). EDTA is a synthetic chelator of
269 metal cations, with affinities following the sequence of $Fe^{3+} > Cu^{2+} >> Zn^{2+} > Fe^{2+} > Mn^{2+} >>$
270 $Mg^{2+} > Ca^{2+}$ (Norvell, 1991), expected to mobilize the readily available fraction of transition metal
271 cations from cell walls and other apoplastic binding sites.

272 Carrying out the infiltration-centrifugation protocol with insufficient caution can damage cell
273 integrity, thus causing cytoplasmic contamination of the AWF. Therefore, we generated additional
274 control samples in which we provoked cytoplasmic contamination by intentionally inflicting
275 mechanical stress on the leaves during the experimental procedure at three levels of severity (little,
276 intermediate, and strong). A principal component analysis (PCA) of the ionomic profiles of all
277 AWF samples demonstrated that provoked cytoplasmic contamination is associated with strongly
278 elevated concentrations of calcium (Ca), potassium (K), magnesium (Mg), sulfur (S), and
279 phosphorus (P) (Fig. S4a). Consequently, a PCA of ionomic profiles is a sensitive means to
280 identify cytoplasmically contaminated AWF samples, all of which were excluded from further
281 analysis (Fig. S4a and B).

282 Compared to total concentrations across entire hydrated leaves, nutrients (Fe, Mo, Cu, Ca, S, P,
283 Mg, and K) were generally depleted in AF, most strongly for Fe (Fig. 1d, see also Fig. S4c and d).
284 By comparison to bulk leaves, there was an enrichment in AF of Mn, Cd and Zn, consistent with
285 the preferential sequestration of these elements in the apoplastic compartment. Overall, only a
286 minor proportion of the total amount of all elements was extracted from leaves in the AWF (Table
287 S7). We calculated Cd and Zn concentrations in AF_{EDTA} to be at least 0.07 and 5.2 µM, and up to
288 0.4 and 40 µM, respectively, with considerable variability between replicate samples and
289 independent experiments (Table S5, Fig. 1e, Fig. S4e-g). Accordingly, the range of Zn

290 concentrations in the AF included concentrations capable of preventing the growth of the most
291 sensitive phyllosphere bacterial strains when tested on solid R2A medium. Cd concentrations in
292 AF closely approached these magnitudes (Table 1; Fig. 1E), although plants were grown on
293 greenhouse soil containing only trace levels of Cd (total Cd < 0.1 mg kg^{-1}; Table S6). Cd and Zn
294 concentrations in AF were elevated in the presence of EDTA in the IF, suggesting that EDTA
295 either prevented immobilization or mobilized pools of both metals from extracellular binding sites
296 within infiltrated leaves (Fig. 1e, Table S5, Fig. S4a). It should be noted that we consider the direct
297 quantitative comparison between metal concentrations in AF and R2A medium merely as a first
298 reasonable approximation (see also Discussion).

299 In contrast to Cd and Zn, total concentrations of Cu and Mn in the AF of approximately 1 and 70
300 µM, respectively, were clearly below toxic levels in the R2A medium between 10 and 100 µM
301 Cu^{II} and 1 to 2 mM Mn^{II} (Dataset S1, Fig. 1a, Table 1). Overall, Cu concentrations in AF were
302 independent of whether we used EDTA solution or water as IF, suggesting that negligible
303 proportions of the apoplastic Cu pool were reversibly bound to cell walls of infiltrated leaves (Fig.
304 1d, Fig. S4g, Table S5). In summary, these results indicated that Cd and Zn are enriched in the leaf
305 apoplast and have the potential to directly attenuate the growth of a subset of phyllosphere bacteria.

306 **Towards extrapolating how metals affect phyllosphere bacterial community composition**

307 Previous work demonstrated that the absence of single bacterial strains, such as L203-
308 *Microbacterium*, L231-*Sphingomonas*, L233-*Rhodococcus,* and L262-*Rhizobium*, can alter the
309 structures of bacterial communities (Carlström *et al.*, 2019). In these so-called keystone strains,
310 maximum permissive concentration (MPC) was often larger or equal to *At*-LSPHERE-wide EC_{50},
311 however, with strain-specific sensitivities to individual metal(loid)s, so that none of these strains
312 shared an identical profile with any other strain (Fig. 2a, Dataset S1). This suggested that
313 metal(loid) tolerances in keystone strains reflect distinct evolutionary histories rather than shared
314 responses to chemical stress. L233 was the most Cd-sensitive, with an MPC of 1.5 µM Cd
315 (compare Fig. 2a, Table 1), for instance. Although the maximal Cd concentration in AF (0.4 µM)
316 was lower by comparison (see Fig. 1e, Table S5), we observed in liquid R2A medium that a
317 concentration of 0.5 µM Cd suppressed the growth of L203, L231 and L233 (Table S8 and S9).

318 Next, we tested for possible combined effects of metals on the keystone strains. We examined the
319 effects of combining Cd^{II} and Cu^{II}, and of combining Cd^{II}, Zn^{II}, and Mn^{II} in the liquid culture

320 system (Fig. 2b and c). A mild growth reduction appeared at concentrations of 0.5 μM Cd^{II} or 100
321 μM Cu^{II}, whereas the combination of 0.5 μM Cd^{II} and 100 μM Cu^{II} completely eliminated the
322 growth of L233, thus implying synergistic toxicity of Cd^{II} and Cu^{II} (Fig. 2b, Table S8). Similarly,
323 neither Cd^{II} nor Cu^{II} alone were heavily toxic to L262 at the tested concentrations, whereas the
324 combination of 100 μM Cu^{II} with any of the tested Cd^{II} concentrations exacerbated the toxic
325 effects. In contrast, combined treatments appeared to alleviate toxicity in L231 when compared to
326 treatments with Cd^{II} and Cu^{II} alone (Fig. 2b, Table S8). Reproducible combined effects were
327 largely restricted to Cu^{II} concentrations in liquid R2A media that were 14- to 300-fold higher than
328 in AF (see Table S5).

329 In experiments combining up to three metals, the single Zn^{II} concentration tested (50 μM) alone
330 tended to decrease the growth of L203 and L231, and more strongly of L233 and L262 (Table S9).
331 The tested Mn^{II} concentration (10 μM) alone had no consistent effects on the growth of keystone
332 strains (Table S9). When tested in combination with varying concentrations of Cd^{II} (0.5, 5 and 20
333 μM), Zn^{II} exacerbated the toxicity of all Cd^{II} conditions in strain L262, which was highly tolerant
334 to Cd alone, whereas Mn^{II} alleviated both the single and combined toxicities of Zn^{II} and Cd^{II} in
335 this strain (Fig. 2c). Zn^{II} toxicity tended to increase in combination with Cd^{II} in L231 and in
336 combination with Mn^{II} in L203. Overall, toxicity-alleviating effects of Mn^{II} tended to predominate,
337 including its effects on L233 and L203 suffering from Cd^{II} toxicity (0.5 μM) or exposed to a
338 combination of Cd^{II} and Zn^{II}, but the sizes of these effects were mostly small and insufficient to
339 rescue growth of the same strains at the next higher tested concentration of 5 μM Cd, for instance
340 (Table S9). In summary, these experiments suggested that combined effects are unlikely to cause
341 major increases in metal tolerances of strains compared to single metals as shown in Fig. 1a.

342 **Phylogeny at the genus level explains most of the variation in metal tolerance profiles**

343 Next, we examined metal tolerance profiles in relation to the phylogeny of *At*-LSPHERE strains.
344 *Actinobacteria* were significantly depleted by Cd concentrations of ≥ 15 μM and enriched among
345 the strains that continued to grow at ≥ 0.2 mM Cu and ≥ 0.4 mM Zn, when compared to other
346 classes (Fig. 3). Relative to other classes, Gammaproteobacteria were enriched at high levels of ≥
347 2.5 mM arsenite. Hierarchical clustering of MPCs identified 10 distinct clusters of bacterial strains
348 sharing similar metal(loid) tolerance profiles (Fig. 4).

349 Cluster I comprised only three strains, L92-*Methylobacterium*, L396-*Bradyrhizobium*, and L401-
350 *Bradyrhizobium* (all α-Proteobacteria), which were highly tolerant to multiple metals but not to
351 the metalloid arsenite. These strains were the most Cd-tolerant (1.5 mM) and tolerated more than
352 twice the EC_{50} concentrations of Cu, Zn, and Mn (Fig. 4, Dataset S1). Cluster II consisted of five
353 highly Zn- and Cu-tolerant strains. Strains highly tolerant to arsenite grouped in cluster III, highly
354 Mn-tolerant strains in cluster IV, and highly Mn-tolerant and Cu-sensitive strains in cluster V.
355 Cluster VI comprised highly to moderately Cu-tolerant strains, some of which were also highly
356 Cd-tolerant. Clusters VII and VIII contained strains with intermediate Cu tolerance, whereby
357 cluster VII contained arsenite-sensitive and cluster VIII contained moderately arsenite-tolerant
358 strains. The final two clusters, IX and X, grouped strains that were highly Cu-sensitive and
359 sensitive to most other metal(loid)s, with intermediate tolerance to arsenite in cluster IX and
360 sensitivity to arsenite in cluster X. Metal tolerance profiles were similar within the genus
361 *Rhizobium*, of which approximately 73% grouped in Cluster X, and 13% in clusters V and IX,
362 respectively. In contrast, the seven *Rhodococcus* strains were distributed into four different
363 clusters: one strain in cluster III, two strains in the neighboring cluster VII, three strains in cluster
364 VIII, with two directly next to one another and a third one further away, and finally one strain in
365 cluster X. Similarly, the nine *Pseudomonas* strains were spread across the five clusters V and VII
366 to X, whereby only two of them clustered next to one another in cluster V. These patterns suggested
367 that phylogenetic relationships account for only part of the variation in metal tolerance profiles.

368 To obtain more quantitative information on the contribution of phylogeny to the variation in metal
369 tolerance we employed dimensionality reduction-based analyses. There were no major differences
370 between strains of different taxonomic classes according to a PCA of strain-wise MPCs (Fig. S6a),
371 and a constrained principal coordinate analysis (CPCoA) constrained by class explained only 6%
372 of the variance (Fig. S6b; $p < 0.05$). By contrast, CPCoA attributed 42% of the variance to genus
373 (Fig. S6c; constrained by genus, $p < 0.001$). In agreement with this, a representation of metal
374 tolerances on a phylogenetic tree based on 16S rRNA DNA sequences (Bai et al. 2015) suggested
375 that closely related strains mostly exhibited similar metal tolerance profiles (Fig. 5). For example,
376 *Methylobacterium* strains L90, L92, L119, L121, L122, and L123 were highly Cd tolerant, and
377 *Methylobacterium* L90, L92, and L122 were Cu- and Zn-tolerant (Fig. 5). Similarly, all *Bacillus*
378 strains were sensitive to Cd and Cu, and all *Rhizobium* strains (Alphaproteobacteria) were sensitive
379 to Cu and Zn. In summary, metal(loid) tolerance profiles were diverse and partially followed

380 phylogenetic relationships, most prominently at the genus level, suggesting that the remaining
381 phenotypic variation among *At*-LSPHERE strains reflects recent evolutionary divergence.

382 **Genetic basis of differential metal tolerances among bacterial strains**

383 We investigated whether molecular mechanisms that were previously characterized in bacteria can
384 explain between-strain variation in metal tolerances. First, we conducted a PCA of strain-wise
385 MPC for Cd and the orthologs of 9 genes described in the literature to increase Cd tolerance that
386 were present in the genome of each strain (Fig. 6a, Dataset S2). PC 1 clustered the classes
387 *Actinobacteria* and *Bacilli*, which were comparably Cd-sensitive (see Figs. 3 and 5), together
388 towards one side. PC loadings suggested a relationship between enhanced Cd tolerance and the
389 presence of *czcA, czcB, czcC, czcD*, *smtA*, and *tolC*, of *zntA* for PC1 only, as well as the absence
390 of *zntR* and *cadC..smtB* (Fig. 6a). Beyond the identity of Cd tolerance genes, their gene dosage (or
391 copy number) could be expected to scale with strain-level Cd tolerance. A Kendall's rank
392 correlation analysis of the gene score, which we calculated as the cumulative number of Cd
393 tolerance-related genes and gene copies present in the genome, and Cd MPC showed a significant
394 correlation ($\tau = 0.31$, $p < 3.5 \times 10^{-9}$; Fig. 6b).

395 We next broadened our analysis to include known metal(loid)-related (100 genes of interest, GoI,
396 Dataset S2). CPCoA indicated that 22% of the presence/absence genetic variation for these genes
397 was explained by class (constrained by class, $p \leq 0.001$), and 63% by genus (constrained by genus,
398 $p \leq 0.001$) (Fig. S7a-c). This result further highlighted the importance of genus-level taxonomy,
399 consistent with the pattern observed for phenotypic variation in metal tolerances (Fig. S6). By
400 comparing median MPC of all strains containing the GoI in their genomes with that of all strains
401 lacking the GoI (Datasets S3 and S4), we identified 51 genes that were significantly associated
402 with tolerance to one or several metal(loid)s: 21 genes (41%) for Cd, 9 for Cu (18%), 15 (29%)
403 for Zn, none for As^{III}, 20 (39%) for Mn, and 9 (18%) for As^{V} tolerance (Table S10, Dataset S4,
404 Wilcox rank-sum test, *p*-values adjusted with Holm-Bonferroni corrections). We detected positive
405 effects for *czcA, czcB, czcC, tolC* and *zntA* on Cd tolerance, in agreement with Fig. 6a, whereby
406 statistical significances were the highest for *czcA*, *czcB* and *tolC* (Dataset S4, Fig. 7, $p_{adj} < 0.005$).
407 In addition to genes previously implicated in bacterial Cd tolerance, our analysis implicated
408 *arsC1..arsC*, *arsH*, *cusB..silB*, *mdtA*, *mdtB*, *mdtC* and *zur* as candidate genes for increasing Cd
409 tolerance. Conversely, the presence of *comB*, *cmtA*, and *smtB* each decreased the median MPC of

410 Cd by a factor of 40. *Actinobacteria* and *Bacilli* of the *At*-LSPHERE collection were characterized
411 by an overall lack of Cd tolerance genes and the presence of Cd-sensitizing genes, consistent with
412 their Cd sensitivity (Fig. 7, see Figs. 3 to 5 and 6a). Similarly, there was an agreement between Cd
413 tolerance and the genomic content of Cd-related genes identified here in the most Cd-sensitive
414 strains (L454, L172, L263, and L406) and one of the two most highly Cd-tolerant strains (L396)
415 (Fig. 7). As an exception to this pattern, the genome of the highly Cd-tolerant strain L92-
416 *Methylobacterium,* contains only three known Cd tolerance-increasing genes, *czcA, czcB* and *zntA*.
417 Taken together, these results implicate orthologues of previously characterized metal(loid)-related
418 genes in specific metal(loid) tolerances of phyllosphere bacterial strains and suggest further
419 contributions from unknown or poorly annotated genes.

420

421 ## Discussion

422 **Metal tolerances of individual strains and their relevance for bacterial community**
423 **composition in the leaf endosphere**

424 Our results support the conclusion that the levels of Zn and Cd, and possibly also of other
425 metal(loid)s, in the leaf apoplast contribute to shaping bacterial community composition in the leaf
426 endosphere of *A. thaliana* by eliminating or attenuating the growth of sensitive bacterial
427 genotypes. First, we observed marked overall differences in the degrees of tolerance to Zn and Cd
428 between the bacterial strain collection from the phyllosphere and the collection from unplanted
429 soil (Fig. 1, Table 1). This suggests an enrichment of strains exhibiting elevated tolerance to these
430 metals among in the *At*-LSPHERE collection by comparison to the collection from unplanted soil.
431 Second, Zn and Cd concentrations in the leaf apoplastic fluid (AF) of soil-grown Arabidopsis
432 plants closely approached, or overlapped with, the metal concentrations that were toxic to metal-
433 sensitive bacterial strains of the *At*-LSPHERE collection in solid R2A media (Figs. 1 and S4, Table
434 S5). In addition, Cd, Mn and Zn were enriched in AF compared to their concentrations in bulk
435 leaves. Third, two keystone strains (Carlström *et al.*, 2019), L233-*Rhodococcus* and L203-
436 *Microbacterium*, were among the most sensitive strains (Fig. 2 and Fig. S5), implying the potential
437 for pronounced secondary effects of Zn and Cd toxicity on overall species composition in the leaf
438 endosphere. Finally, a set of exemplary tests conducted by us suggested that between-strain and

439 between-metal interactions had no, or only few, and mostly small, reproducible effects alleviating
440 Zn or Cd toxicity (Figs. 1 and 2, S2 and S3, Tables S8 and S9).

441 Our study has some limitations that should be considered when interpreting these conclusions.
442 While partly shared soil environments of origin support the comparability of the bacterial
443 collections (Bai *et al.*, 2015), the number of strains was considerably smaller in the soil collection
444 than in the *At*-LSPHERE collection, thus potentially decreasing the precision of the values
445 summarizing metal(loid) tolerances across soil bacterial strains (Fig. 1). Relating metal
446 concentrations in leaf AF to those in solid or liquid bacterial growth media fundamentally remains
447 an extrapolation. Considerable proportions of the total metal concentrations accessible to and
448 measured in AF, as well as those measured in R2A media, are present in chelated form in solution,
449 within precipitates or bound to the surfaces of solids. Yet, the degree of Cd and Zn toxicity to
450 bacteria is likely to depend on the concentrations of their free aqueous cations. In addition to this,
451 the levels of other solutes can strongly influence metal toxicity. Importantly, other divalent cations
452 compete with toxic metal cations for bacterial uptake, and the levels of bioavailable nutrients, such
453 as phosphate, sulfur, iron and manganese, can alleviate metal toxicity inside bacterial cells. The
454 overall elemental composition of solid R2A media (*ca*. 5-fold Fe, 10% Ca, 30% Mg, 20% K, 6-
455 fold S, and 2.6-fold P, compared to AF) suggested that bacterial metal toxicities are broadly
456 comparable between the two matrices (Table S5). The agar polysaccharide in solid R2A medium
457 contributes a macromolecular matrix of metal cation binding sites, similar to the cell walls of
458 Arabidopsis which interact with the AF *in vivo*. Agar also contributes substantial quantities of
459 contaminant Ca^{2+} and Mg^{2+} cations capable of competing with Cd^{2+} and Zn^{2+}, compared to liquid
460 R2A media (Table S3). Thus, unsurprisingly, bacteria generally tolerated higher Cd concentrations
461 in solid than in liquid R2A medium (≥ 16-fold difference for L262 and the intermediate SynCom,
462 > 10-fold for L203; compare Fig. 1c with Fig. S2, Fig. 2a with Suppl. Fig. S5).

463 We expect the composition of leaf AF to be highly dynamic, which must be kept in mind when
464 comparing with the metal concentrations in our bacterial tolerance assays. In addition to the
465 concentrations of free metal cations and other contributing factors outlined above, a pH decrease
466 (Geilfus, 2017; Geilfus *et al.*, 2020) and a more oxidized redox state can directly enhance metal
467 toxicity in AF by decreasing the proportion of metal cations in complexed or bound from, thereby
468 increasing the bioavailable fraction of free aqueous metal cations. Importantly, in response to
469 infection by the necrotrophic fungus *Plectosphaerella cucumerina*, Arabidopsis accumulated Zn^{2+}

470 in the leaf apoplast dependent on the Zn^{2+}/Cd^{2+} efflux pump-encoding genes *AtHMA2* and
471 *AtHMA4* (Escudero *et al.*, 2022). Thus, microbe-induced fluxes of metal cations across the plasma
472 membrane of plant cells may be more widespread than is currently recognized. Interpreting the
473 differences in overall metal tolerances of the *At*-LSHERE collection compared to soil bacterial
474 communities as an outcome of selective strain enrichment would imply that in phyllosphere
475 bacterial communities even the mildest Zn and Cd toxicities are ecologically relevant (compare
476 EC_5 in Table 1). We observed the largest relative differences between *At*-LSPHERE and soil
477 bacterial Zn and Cd tolerances for EC_{95} (Table 1). One possible interpretation of these observations
478 could be that the corresponding metal levels are ecologically relevant for Zn^{II} (corresponding to
479 the degree of toxicity inflicted by 0.66 to 5.6 mM Zn in solid R2A medium), Cd^{II} (0.054 to 0.56
480 mM Cd) and possibly also Cu^{II} (1.4 to 1.6 mM Cu^{II}).

481 In contrast to Zn, Cd has no known nutritional role in Arabidopsis, raising the question of
482 acquisition and partitioning of Cd by plants in conjunction with a possible biological role in plant-
483 microbe interactions suggested by our results. In addition to HMA2 and HMA4, and among other
484 characterized membrane transporters (Sterckeman & Thomine, 2020), Cd^{2+} is a secondary
485 substrate of the high-affinity root Fe^{2+} uptake systems IRT1 of Arabidopsis and RIT1 of pea
486 (Connolly *et al.*, 2002; Vert *et al.*, 2002; Cohen *et al.*, 2004). In the Zn- and Cd-hyperaccumulating
487 species *Arabidopsis halleri* and *Noccaea caerulescens*, extremely high concentrations above 3 mg
488 g^{-1} Zn and 0.1 mg g^{-1} Cd in bulk leaf dry biomass are thought to function as elemental defenses
489 against biotic stress, including bacterial pathogens (Fones *et al.*, 2010; Hörger *et al.*, 2013;
490 Kazemi-Dinan *et al.*, 2014; Stein *et al.*, 2017). Maximal Zn and Cd concentrations in leaves of
491 healthy *A. thaliana* plants are less than 10% by comparison, but this does not preclude the
492 possibility of a highly localized accumulation of Zn or Cd to levels that can be toxic for bacteria.
493 Much higher bacterial toxicity of Cd compared to Zn (Table 1), as well as the absence of a
494 correlation between Cd and Zn tolerance among *At*-LSPHERE strains (Fig. 4), argue against the
495 possibility that our findings could be a consequence of the similarity between the chemical
496 properties of Cd and Zn.

497 For metal(loid)s other than Zn and Cd, there was substantially less evidence for a role in shaping
498 phyllosphere microbial communities. Cu^{II} concentrations in AF were far below Cu^{II} levels toxic
499 for *At*-LSPHERE bacteria on agar-solidified media, and *At*-LSPHERE bacteria were not generally
500 more Cu^{II}-tolerant than soil bacteria (Fig. 1). Cd toxicity to the keystone strains L233-

501 *Rhodococcus* and L262-*Rhizobium* was potentiated by the additional presence of Cu^{II} only at a
502 high concentration of 100 µM in liquid R2A medium (Fig. 2). However, some existing knowledge
503 supports that Cu could be relevant in plant-microbe interactions. Human macrophages mediate the
504 local accumulation of Cu ions in the phagolysosome to kill pathogens (White *et al.*, 2009; Achard
505 *et al.*, 2012; Samanovic *et al.*, 2012). Transcript profiling revealed that several copper-related
506 genes were upregulated in *A. thaliana* leaves in response to the strain *Methylobacterium*
507 *extorquens* PA1 (Vogel *et al.*, 2016), and the treatment of Arabidopsis with Cu was reported to
508 enhance its immunity against *Pseudomonas syringae* pv. *tomato* DC3000, for example (Xia *et al.*,
509 2026). The strongest biotoxic effects of Cu generally result from redox cycling between oxidized
510 Cu^{II} and reduced Cu^{I}, and from exposure to Cu^{I} (Samanovic *et al.*, 2012). Similar to their proposed
511 functions in human immune cells, plasma membrane-localized $gp91^{phox}$ NADPH oxidases, such
512 as the superoxide-producing *At*rbohD and *At*rbohF (Nathan & Shiloh, 2000; Torres *et al.*, 2002)
513 and the Cu^{II} chelate reductases *At*FRO4 and *At*FRO5 (Bernal *et al.*, 2012), could contribute to
514 redox cycling of Cu in the plant phyllosphere. Indeed, *AtrbohD* is important for the maintenance
515 of microbiota in leaves of *A. thaliana* (Pfeilmeier *et al.*, 2021). Total As was below our detection
516 limits in AWF, and bacteria seemed to be comparably tolerant to arsenite (As^{III}) and arsenate (As^{V})
517 on solid R2A medium. Organo-arsenicals, which can be far more toxic than inorganic forms of
518 As, warrant further investigation, given that *A. thaliana* can take up dimethylarsenate and convert
519 it into dimethylmonothioarsenate- and dimethyldithioarsenate, for example (Colina Blanco *et al.*,
520 2023). For Mn and As^{III}, only EC_5 values were higher in the *At*-LSPHERE than in the soil bacterial
521 collection, implying a possible ecological relevance associated with mildly toxic concentrations in
522 AF (Table 1), which will require further work. The finding that Mn^{II} alleviated Cd^{II} toxicity in
523 keystone strain L203-*Microbacterium* in liquid R2A media may be related to this (Fig. 2).

524 To date, the information available from previous metal(loid) tolerance screens of bacterial strain
525 collections is limited. Much of the available data are from single bacteria hypothesized to exhibit
526 enhanced metal(loid) tolerance (Tada & Inoue, 2000; Zhao *et al.*, 2015), and from multiple strains
527 collected in environments characterized by high levels of abiotic stress or heavy metals (Nieto *et*
528 *al.*, 1987; Idris *et al.*, 2004; Abou-Shanab *et al.*, 2007; Barzanti *et al.*, 2007; Fones *et al.*, 2010;
529 Luo *et al.*, 2011; Fones *et al.*, 2016). Overall, these studies concur with our results regarding the
530 comparably high toxicity of Cd and the overall narrow concentration range for Cu^{II} (see Table 1,
531 Fig. 1). Although *Actinobacteria* were the least Cd-tolerant among *At*-LSPHERE strains, a study

532 of heavy metal-tolerant *Actinobacteria* identified strains able to tolerate Cd and Cu concentrations
533 of up to 100 mM, i.e., about 70- and 100-fold higher concentrations than the most tolerant strains
534 of the *At*-LSPHERE collection (Amoroso *et al.*, 1998). Across these previous studies, natural
535 variation in bacterial metal tolerances is very large, and the environment of bacterial origin appears
536 to be more influential than their phylogeny. Metal tolerances of *At*-LSPHERE strains were mostly
537 lower than those reported in bacteria originating from metal-rich environments, with some
538 remaining uncertainty given the diversity of media and designs among tolerance assays used.

539 **Relationship of metal(loid) tolerance with phylogeny and the gene content of bacterial**
540 **genomes**

541 Phylogenetically closely related bacteria generally tended to exhibit similar metal tolerance
542 profiles, and our results supported a genetic basis of differential metal tolerance profiles, despite a
543 few notable exceptions (Figs. 4 to 7), consistent with previous findings among bacterial leaf
544 endophytes of metal hyperaccumulator plants (Fones *et al.*, 2010; Fones *et al.*, 2016). We
545 identified some candidate genes in *At*-LSPHERE strains among the genes annotated as orthologues
546 of metal(loid)-related based on previous work in bacterial models (Figs. 7, Table S10). Of the
547 genes strongly implicated in Cd tolerance in the *At*-LSPHERE collection, the *czc* and *znt* operons
548 are well-known (Figs. 6 and 7, Table S10, Dataset S4). The CzcCBA efflux system of *Ralstonia*
549 *metallidurans* pumps Cd out of cells (Nies *et al.*, 1989; Nies & Silver, 1989; Nies, 1992b) for Cd
550 resistance (Nies, 1992a; Silver & Walderhaug, 1992), supported by a virtual model of *R.*
551 *metallidurans* (Legatzki *et al.*, 2003). Bacterial ZntA Zn/Cd/Pb-transporting P-type ATPase
552 proteins often function in Zn detoxification and can be relevant for Cd resistance (Beard *et al.*,
553 1997; Rensing *et al.*, 1997; Outten *et al.*, 1999; Singh *et al.*, 1999; Choudhury & Srivastava, 2001;
554 Chaoprasid *et al.*, 2015). A low concentration of Cd (50 µM) completely inhibited growth of an
555 *Agrobacterium tumefaciens* C58 loss-of-function *zntA* mutant (Chaoprasid *et al.*, 2015). We did
556 not identify the gene encoding the known regulator of *zntA*, *zntR* (Table S10), and its presence
557 even appeared to be inversely related to Cd tolerance (Fig. 6), which might reflect mutual
558 interference between the toxin Cd^{2+} and the micronutrient Zn^{2+}.

559 In addition to known Cd tolerance mechanisms, our data implicated Resistance-Nodulation-
560 Division (RND) type multidrug efflux pump component-encoding *mdtA*, *B*, and *C* in Cd tolerance
561 of *At*-LSPHERE bacteria. In *Escherichia coli*, periplasmic MdtA connects the inner membrane

562 efflux pump MdtBC to the outer membrane channel TolC to confer antibiotic resistance
563 (Nagakubo *et al.*, 2002; Nishino *et al.*, 2007; Kim *et al.*, 2010). The fourth gene of the *mdtABCD*
564 operon *mdtD* encodes a putative transporter MdtD, which is also involved in antibiotic resistance
565 and can promote the efflux of citrate, later renamed iron-citrate efflux Transporter IceT in
566 *Salmonella typhimurium* (Frawley *et al.*, 2013). A knockout of *tolC* in *E. coli* resulted in Cd
567 hypersensitivity (Achard-Joris *et al.*, 2005). Moreover, mRNA of genes encoding the AcrAB-TolC
568 efflux pump (*acrB* and *tolC*) were upregulated in Cd-adapted *Salmonella* Typhi Ty2 cells (Kaur
569 *et al.*, 2021). The MdtABC system was implicated in Zn and Cu tolerance in *Salmonella enterica*
570 (Nishino *et al.*, 2007). Supporting the *in planta* relevance of RND-type efflux systems, an RND
571 family efflux transporter MFP subunit (Mext_2832) was detected in the *in planta* proteome of *M.*
572 *extorquens* PA1 (Müller *et al.*, 2016a), and efflux systems including CzcABC family RND
573 transporters were among the proteins induced during phyllosphere colonization in *Rhizobium* L68
574 and *Sphingomonas* L257 (Hemmerle *et al.*, 2022).

575 Our results implicated genes with known roles in As tolerance, *arsC1..arsC* and *arsH*, in Cd
576 tolerance of *At*-LSPHERE strains (Figs. 6 and 7, Table S10, Dataset S4). Among three different
577 KO identifiers linked to *arsC* (*arsC1..arsC*, K00537; *arsC2..arsC*; K03741, *arsC*, K18701;
578 Dataset S4), only *arsC1..arsC* (*arsC1*), described as arsenate reductase that uses glutathione as a
579 cofactor (glutaredoxin) in the KEGG database, showed a positive effect on Cd tolerance. Dhankher
580 *et al.* (2003) reported that bacterial *arsC1* conferred Cd tolerance to *E. coli*, and to *A. thaliana* and
581 *Nicotiana tabacum* plants, but the underlying mechanism remains unidentified. The second Cd
582 tolerance candidate gene in the *ars* operon, *arsH* was described as a methylarsenite oxidase that
583 can form the less toxic methylarsenate (Yang & Rosen, 2016) and as an H_2O_2-producing enzyme
584 that can alleviate oxidative stress in *Synechocystis* PCC 6803 (Lopez-Maury *et al.*, 2003). In
585 *Pseudomonas chenduensis* strain MBR, *arsH* transcript levels were upregulated under Cd toxicity
586 (Li *et al.*, 2020). There is no published information on roles in Cd tolerance for the two remaining
587 Cd tolerance candidate genes, *cusB* (annotated to encode a component of a Cu^+ detoxification
588 system), and *zur* (encoding a Zn sensor mediating the transcriptional repression of genes encoding
589 high-affinity Zn uptake systems in its Zn^{2+}-bound form). Effective repression of Zn^{2+} uptake may
590 help to decrease inadvertent uptake of Cd^{2+}. We detected no effect for *cadC..smtB*, which was
591 previously implicated in bacterial Cd tolerance (Endo & Silver, 1995).

592 Future work should test further the hypothesis supported by our results that apoplastic Zn and Cd
593 contribute to the structuring of bacterial communities in the leaf endosphere of *A. thaliana*, as well
594 as investigate the roles of physiologically relevant chemical forms of Cu and As that could not be
595 tested here. What currently remains limiting is the lack of cell biology tools for quantitatively
596 monitoring the dynamics in apoplastic free metal cation concentrations, and of genetic tools for
597 changing these without affecting other aspects of plant metal homeostasis that could have indirect
598 effects on microbial performance. The future exclusion of epiphytic bacteria may facilitate the
599 analysis of interactions between the plant host and bacteria in the leaf endosphere (Chen *et al.*,
600 2020). Finally, functional studies can now target metal(loid) tolerance candidate genes identified
601 here in the published genomes of *At*-LSPHERE bacteria.

602

603 **Acknowledgements**

604 We thank Prof. Dr. Julia Bandow for access to 96-pin microplate replicator. We thank Andreas
605 Aufermann, Rebekka Fresen and Martin Pullack for assistance with plant cultivation and Petra
606 Düchting for contributing her expertise and for conducting all multi-element analyses.

607

608 **Competing Interests**

609 The authors declare no competing interests.

610

611 **Author Contributions**

612 U.K. conceived the project, J.F.P.-M. and U.K. designed research with contributions from J.A.V.,
613 J.F.P.-M. and A.T. performed experiments, J.A.V. contributed materials, J.F.P.-M., A.T., and U.K.
614 analyzed data, J.F.P.-M. and U.K. wrote the manuscript, with contributions from J.A.V. All
615 authors read and edited the manuscript.

616

617 **Data Availability**

618 The data associated with this manuscript are provided in the manuscript or in the Supporting
619 Information. Any additional raw data will be made available by the authors upon reasonable
620 request.

621

622 Figure legends

623 **Figure 1. Metal(loid) tolerances of phyllosphere bacterial strains in relation to the leaf**
624 **apoplastic fluid ionome of *A. thaliana*. (a, b)** Metal(loid) dose-response curves for the
625 phyllosphere bacterial collection (a, *At*-LSPHERE, n = 224 strains) and for a bacterial strain
626 collection from unplanted soils (b, n = 33) (Bai et al. 2015). Each strain was spotted on agar-
627 solidified R2A medium supplemented with a series of metal(loid) concentrations. Replicate data
628 points represent independent experiments; lines are curve fits (see Methods, Dataset S1). **(c)** Cd
629 tolerance of synthetic bacterial communities (SynComs; datapoints shown by circles, bars mark
630 mean ± SD, n = 6 technical replicates; data from one experiment representative of a total of four
631 independent experiments). Apparent doubling times of the SynComs were calculated based on the
632 earliest identifiable log phase of growth from time series of OD_{600} measurements with cultivation
633 at 26°C for 24 h (see Fig. S3). ∞: no growth. Note that the horizontal axis is not scaled. **(d)** Ionome
634 of leaf apoplastic fluid (AF_{EDTA}, blue line), and of the entire fresh leaf ($Leaf_{Total}$, red line). Shown
635 is the average (line) and the standard deviation (shadow) for each element as Log_{10} of the
636 concentration ([mM] for Ca, S, P, Mg, and K; [µM] for Zn, Mo, Mn, Fe, Cu, and Cd; n = 4 samples
637 for AF and n = 3 samples for leaves). **(e)** Boxplots showing metal concentrations in apoplastic
638 fluid (AF_{EDTA}, AF_{Water}: extracted in 100 µM EDTA and in water, respectively) of soil-grown
639 plants, alongside metal tolerance of the *At*-LSPHERE collection (re-plotted from (a)). For AF,
640 boxes show median (central line), 25%/75%ile (box), and maximum/minimum (bars) of all
641 measurements (n = 17; see Table S5, Fig. S4e-g). For metal tolerances, boxes show effective
642 concentration EC_{50} (central line), EC_{25}/EC_{75} (boxes) and EC_1/EC_{99} (bars)(see Table 1, and
643 Materials and Methods). Dose-response curves are from a minimum of 3 independent experiments
644 conducted on R2A medium (a, b). AF data are from one representative experiment (d; Table S5,
645 GHs 4; Fig. S4e-g, E4) and from 4 independent experiments conducted on greenhouse soil (e).
646 Not shown: AF_{Water} for Cd and data for As were below our detection limits (d, e).

647 **Figure 2. Metal(loid) tolerance profiles of keystone strains of the *A. thaliana* phyllosphere**
648 **bacterial community**. **(a)** Profiles of maximum permissive concentrations (MPC) normalized to
649 EC_{50} on solid R2A media. Shown are median values (connected by black lines), with minima and
650 maxima (grey shadows, n = 3 independent experiments), on a Log_{10} scale (1 reflects an MPC
651 equivalent to EC_{50}, see Table 1, Dataset S1). Values below 0.5 (small red)/0.05 (large red) and
652 above 5 (small blue) are shown as colored circular shapes. Mn is not shown because of its low
653 toxicity in these strains. **(b, c)** Combined toxicity effects of Cd and Cu (b), and Cd, Zn, and Mn
654 (c) on keystone strains in liquid R2A media (see Tables S8 and S9). Symbols show combined
655 toxicity-enhancing (+) and toxicity-alleviating (-) effects of the metals connected by the
656 corresponding black line; numbers are concentrations [µM]. Results reproduced in three/two out
657 of three independent experiments are shown in black/grey color. Grey dotted lines: effect of the
658 adjacent metal on the combined toxicity of the other two metals (c). Data not shown (n.e.: results
659 could not be evaluated because of metal sensitivity, b). Circle sizes adjusted to fit.

660 **Figure 3. Effects of metal(loid) tolerances of *At*-LSPHERE bacterial strains on the**
661 **phylogenetic structure among the survivors.** Pie fractions reflect the percentage share (with the
662 number given in white) out of all bacterial strains that were able to grow under a given condition
663 (Dataset S1). The metal(loid) concentration is given in black fonts above the chart for each
664 treatment. Asterisks mark significant enrichment (*, black) or depletion (*, white) compared to the
665 control condition (Fisher's exact test, *q-value* < 0.05).

666 **Figure 4. Hierarchical clustering of strains according to their metal(loid) tolerance profiles.**
667 Maximum permissive concentrations of Cd, Zn, Cu, arsenite, and Mn in the *At*-LSPHERE strains
668 (Dataset S1) were clustered by Euclidean distance-based (Ward) clustering (*z*-score-based).
669 Clusters (I to X) are emphasized by different colors (left) and separated by horizontal lines.
670 Symbols mark the positions of *Rhodococcus (n* = 6), *Pseudomonas* (*n* = 9), *Rhizobium* (*n* = 15),
671 and keystone strains (*n* = 4).

672 **Figure 5. Strain-specific metal(loid) tolerances shown over the phylogeny of the *At*-**
673 **LSPHERE strain collection.** Cladogram of the *At*-LSPHERE strain collection (*n* = 214; 16s
674 rRNA-based (Bai et al. 2015)) with circular heatmap representations of relative tolerance.
675 Heatmap color shade reflects strain-wise maximum permissive concentrations (MPC, median of *n*
676 = 3 independent experiments; Dataset S1) normalized to the EC_{50}, the concentration eliminating

677 the growth of 50% of all bacterial strains (Cd: 0.049 mM, Zn: 0.5 mM, Cu: 0.4 mM, As^{III}: 1.1 mM,
678 Mn: 9.2 mM; Table 1). Strains (n = 8) not profiled for metal tolerance are marked by a black line
679 around the colored circle.

680 **Figure 6. Relationships between known Cd tolerance genes and Cd tolerance of *At*-**
681 **LSPHERE strains. (a)** PCA of strain-wise maximum permissive Cd concentrations (MPC, *z*-
682 score-based) and presence/absence of known Cd tolerance-related genes. Each datapoint
683 represents one strain (Datasets S1-S3). The percentages of variation accounted for by each
684 significant PC are given in parentheses (95% confidence intervals: PC 1, 31% to 36.7%; PC 2,
685 10.9% to 13.8%; bootstrapping with 999 replicates). KEGG Orthology (KO) identifiers with
686 significant loadings on PC1 are: *czcA–D* and *tolC* (alternative short names linked by "..."; Dataset
687 S6). **(b)** Plot of strain-wise maximum permissive Cd concentration (MPC, absolute) against a gene
688 score incorporating both presence/absence and copy number of known Cd tolerance-related genes.
689 Each datapoint represents one strain (Datasets S1-S3). The gene score of a strain is the genome-
690 wide sum of genes and gene copies with previously published roles in Cd tolerance (Kendall's rank
691 correlation, $\tau = 0.31$, $p = 3.5\times10^{-9}$; Dataset S7).

692 **Figure 7. Metal(loid)-related genes implicated in Cd tolerance of *At*-LSPHERE strains**
693 **shown over phylogeny.** Shown are known metal(loid)-related genes of which the presence in the
694 genome was statistically associated with altered Cd tolerance in our study ($p_{adj} < 0.005$, for *arsH*
695 $p_{adj} = 0.023$; with Bonferroni corrections). Colors of KO identifiers reflect whether the median of
696 maximum permissive concentrations (MPC median) of all positive strains was > 2-fold higher
697 (red) or > 2-fold lower (blue) than that of all strains lacking an orthologue (Dataset S4; else KO
698 id. not shown). Genes (KO identifiers) are only shown if present in at least 30 bacterial strains
699 (Dataset S4). Strains (n = 8) not profiled for metal tolerance are marked by a black line around the
700 colored circle.

701

References

Abou-Shanab RA, van Berkum P, Angle JS. 2007. Heavy metal resistance and genotypic analysis of metal resistance genes in gram-positive and gram-negative bacteria present in Ni-rich serpentine soil and in the rhizosphere of *Alyssum murale*. *Chemosphere* **68**(2): 360-367.

Achard-Joris M, van den Berg van Saparoea HB, Driessen AJ, Bourdineaud JP. 2005. Heterologously expressed bacterial and human multidrug resistance proteins confer cadmium resistance to *Escherichia coli*. *Biochemistry* **44**(15): 5916-5922.

Achard MES, Stafford SL, Bokil NJ, Chartres J, Bernhardt PV, Schembri MA, Sweet MJ, McEwan AG. 2012. Copper redistribution in murine macrophages in response to Salmonella infection. *Biochem J* **444**(1): 51-57.

Amoroso MJ, Castro GR, Carlino FJ, Romero NC, Hill RT, Oliver G. 1998. Screening of heavy metal-tolerant actinomycetes isolated from the Sali River. *J Gen Appl Microbiol* **44**(2): 129-132.

Andersen TG, Barberon M, Geldner N. 2015. Suberization - the second life of an endodermal cell. *Curr Opin Plant Biol* **28**: 9-15.

Bai Y, Müller DB, Srinivas G, Garrido-Oter R, Potthoff E, Rott M, Dombrowski N, Münch PC, Spaepen S, Remus-Emsermann M, et al. 2015. Functional overlap of the Arabidopsis leaf and root microbiota. *Nature* **528**(7582): 364-369.

Barberon M, Vermeer JE, De Bellis D, Wang P, Naseer S, Andersen TG, Humbel BM, Nawrath C, Takano J, Salt DE, et al. 2016. Adaptation of Root Function by Nutrient-Induced Plasticity of Endodermal Differentiation. *Cell* **164**(3): 447-459.

Barzanti R, Ozino F, Bazzicalupo M, Gabbrielli R, Galardi F, Gonnelli C, Mengoni A. 2007. Isolation and characterization of endophytic bacteria from the nickel hyperaccumulator plant *Alyssum bertolonii*. *Microb Ecol* **53**(2): 306-316.

Beard SJ, Hashim R, MembrilloHernandez J, Hughes MN, Poole RK. 1997. Zinc(II) tolerance in *Escherichia coli* K-12: evidence that the *zntA* gene (o732) encodes a cation transport ATPase. *Mol Microbiol* **25**(5): 883-891.

Bernal M, Casero D, Singh V, Wilson GT, Grande A, Yang H, Dodani SC, Pellegrini M, Huijser P, Connolly EL. 2012. Transcriptome sequencing identifies SPL7-regulated copper acquisition genes FRO4/FRO5 and the copper dependence of iron homeostasis in Arabidopsis. *The Plant Cell* **24**(2): 738-761.

Bulgarelli D, Schlaeppi K, Spaepen S, Ver Loren van Themaat E, Schulze-Lefert P. 2013. Structure and functions of the bacterial microbiota of plants. *Annu Rev Plant Biol* **64**: 807-838.

Carlström CI, Field CM, Bortfeld-Miller M, Müller B, Sunagawa S, Vorholt JA. 2019. Synthetic microbiota reveal priority effects and keystone strains in the Arabidopsis phyllosphere. *Nat Ecol Evol* **3**(10): 1445-1454.

Chandrangsu P, Rensing C, Helmann JD. 2017. Metal homeostasis and resistance in bacteria. *Nat Rev Microbiol* **15**(6): 338-350.

Chaoprasid P, Nookabkaew S, Sukchawalit R, Mongkolsuk S. 2015. Roles of *Agrobacterium tumefaciens* C58 ZntA and ZntB and the transcriptional regulator ZntR in controlling Cd^{2+}/Zn^{2+}/Co^{2+} resistance and the peroxide stress response. *Microbiology* **161**(9): 1730-1740.

Chen T, Nomura K, Wang X, Sohrabi R, Xu J, Yao L, Paasch BC, Ma L, Kremer J, Cheng Y, et al. 2020. A plant genetic network for preventing dysbiosis in the phyllosphere. *Nature* **580**(7805): 653-657.

Choudhury R, Srivastava S. 2001. Zinc resistance mechanisms in bacteria. *Curr Sci* **81**(7): 768-775.

Clemens S. 2001. Molecular mechanisms of plant metal tolerance and homeostasis. *Planta* **212**(4): 475-486.

Cohen CK, Garvin DF, Kochian LV. 2004. Kinetic properties of a micronutrient transporter from *Pisum sativum* indicate a primary function in Fe uptake from the soil. *Planta* **218**(5): 784-792.

Colina Blanco AE, Pischke E, Higa Mori A, Kerl CF, Clemens S, Planer-Friedrich B. 2023. In Planta Arsenic Thiolation in Rice and *Arabidopsis thaliana*. *Environ Sci Technol* **57**(51): 21846-21854.

Connolly EL, Fett JP, Guerinot ML. 2002. Expression of the IRT1 metal transporter is controlled by metals at the levels of transcript and protein accumulation. *Plant Cell* **14**(6): 1347-1357.

Dhankher OP, Shasti NA, Rosen BP, Fuhrmann M, Meagher RB. 2003. Increased cadmium tolerance and accumulation by plants expressing bacterial arsenate reductase. *New Phytol* **159**(2): 431-441.

Endo G, Silver S. 1995. CadC, the transcriptional regulatory protein of the cadmium resistance system of *Staphylococcus aureus* plasmid pI258. *J Bacteriol* **177**(15): 4437-4441.

Escudero V, Castro-León Á, Sánchez DF, Abreu I, Bernal M, Krämer U, Grolimund D, González-Guerrero M, Jordá L. 2022. *Arabidopsis thaliana* Zn^{2+}-efflux ATPases HMA2 and HMA4 are required for resistance to the necrotrophic fungus *Plectosphaerella cucumerina* BMM. *J Exp Bot* **73(1):339-350**.

Farvardin A, Gonzalez-Hernandez AI, Llorens E, Garcia-Agustin P, Scalschi L, Vicedo B. 2020. The Apoplast: A Key Player in Plant Survival. *Antioxidants* **9**(7).

Figueiredo J, Cavaco AR, Guerra-Guimaraes L, Leclercq C, Renaut J, Cunha J, Eiras-Dias J, Cordeiro C, Matos AR, Sousa Silva M, et al. 2021. An apoplastic fluid extraction method for the characterization of grapevine leaves proteome and metabolome from a single sample. *Physiol Plant* **171**(3): 343-357.

Fones H, Davis CA, Rico A, Fang F, Smith JA, Preston GM. 2010. Metal hyperaccumulation armors plants against disease. *PLoS Pathog* **6**(9): e1001093.

Fones H, Preston GM. 2013. The impact of transition metals on bacterial plant disease. *FEMS Microbiol Rev* **37**(4): 495-519.

Fones HN, McCurrach H, Mithani A, Smith JA, Preston GM. 2016. Local adaptation is associated with zinc tolerance in Pseudomonas endophytes of the metal-hyperaccumulator plant *Noccaea caerulescens*. *Proc Biol Sci* **283**(1830).

Frawley ER, Crouch MLV, Bingham-Ramos LK, Robbins HF, Wang WL, Wright GD, Fang FC. 2013. Iron and citrate export by a major facilitator superfamily pump regulates metabolism and stress resistance in *Salmonella typhimurium*. *Proc Natl Acad Sci USA* **110**(29): 12054-12059.

Geilfus C-M. 2017. The pH of the apoplast: dynamic factor with functional impact under stress. *Mol Plant* **10**(11): 1371-1386.

790 **Geilfus C-M, Wang L, Wu J, Xue C. 2020.** The pH of the leaf apoplast is critical for the
791 formation of *Pseudomonas syringae*-induced lesions on leaves of the common bean
792 (*Phaseolus vulgaris*). *Plant Sci* **290**: 110328.
793 **Hemmerle L, Maier BA, Bortfeld-Miller M, Ryback B, Gabelein CG, Ackermann M,**
794 **Vorholt JA. 2022.** Dynamic character displacement among a pair of bacterial
795 phyllosphere commensals *in situ*. *Nat Commun* **13**(1): 2836.
796 **Hörger AC, Fones HN, Preston GM. 2013.** The current status of the elemental defense
797 hypothesis in relation to pathogens. *Front Plant Sci* **4**: 395.
798 **Idris R, Trifonova R, Puschenreiter M, Wenzel WW, Sessitsch A. 2004.** Bacterial
799 communities associated with flowering plants of the Ni hyperaccumulator *Thlaspi*
800 *goesingense*. *Appl Environ Microbiol* **70**(5): 2667-2677.
801 **Inkscape_Project. 2020.** Inkscape. *Retrieved from https://inkscape.org*.
802 **Kajala K, Walker KL, Mitchell GS, Krämer U, Cherry SR, Brady SM. 2019.** Real-time
803 whole-plant dynamics of heavy metal transport in *Arabidopsis halleri* and *Arabidopsis*
804 *thaliana* by gamma-ray imaging. *Plant Direct* **3**(4): e00131.
805 **Kaur UJ, Chopra A, Preet S, Raj K, Kondepudi KK, Gupta V, Rishi P. 2021.** Potential of 1-
806 (1-napthylmethyl)-piperazine, an efflux pump inhibitor against cadmium-induced
807 multidrug resistance in *Salmonella enterica* serovar *typhi* as an adjunct to antibiotics.
808 *Braz J Microbiol* **52**(3): 1303-1313.
809 **Kazemi-Dinan A, Thomaschky S, Stein RJ, Krämer U, Müller C. 2014.** Zinc and cadmium
810 hyperaccumulation act as deterrents towards specialist herbivores and impede the
811 performance of a generalist herbivore. *New Phytol* **202**(2): 628-639.
812 **Kim HS, Nagore D, Nikaido H. 2010.** Multidrug efflux pump MdtBC of *Escherichia coli* is
813 active only as a B2C heterotrimer. *J Bacteriol* **192**(5): 1377-1386.
814 **Krämer U. 2024.** Metal Homeostasis in Land Plants: A Perpetual Balancing Act Beyond the
815 Fulfilment of Metalloproteome Cofactor Demands. *Annu Rev Plant Biol* **75**(1): 27-65.
816 **Küpper H, Lombi E, Zhao FJ, McGrath SP. 2000.** Cellular compartmentation of cadmium
817 and zinc in relation to other elements in the hyperaccumulator *Arabidopsis halleri*. *Planta*
818 **212**(1): 75-84.
819 **Legatzki A, Franke S, Lucke S, Hoffmann T, Anton A, Neumann D, Nies DH. 2003.** First
820 step towards a quantitative model describing Czc-mediated heavy metal resistance in
821 *Ralstonia metallidurans*. *Biodegradation* **14**(2): 153-168.
822 **Li L, Lin Q, Li T, He X, Peng S, Tao Y. 2020.** Transcriptional response of *Pseudomonas*
823 *chenduensis* strain MBR to cadmium toxicity. *Appl Microbiol Biotechnol* **104**(22): 9749-
824 9757.
825 **Lopez-Maury L, Florencio FJ, Reyes JC. 2003.** Arsenic sensing and resistance system in the
826 cyanobacterium *Synechocystis* sp. strain PCC 6803. *J Bacteriol* **185**(18): 5363-5371.
827 **Luo SL, Chen L, Chen JL, Xiao X, Xu TY, Wan Y, Rao C, Liu CB, Liu YT, Lai C, et al.**
828 **2011.** Analysis and characterization of cultivable heavy metal-resistant bacterial
829 endophytes isolated from Cd-hyperaccumulator *Solanum nigrum* L. and their potential
830 use for phytoremediation. *Chemosphere* **85**(7): 1130-1138.
831 **Marschner H, Marschner P. 2012.** *Marschner's mineral nutrition of higher plants*. London ;
832 Waltham, MA: Elsevier/Academic Press.
833 **Müller DB, Schubert OT, Rost H, Aebersold R, Vorholt JA. 2016a.** Systems-level Proteomics
834 of Two Ubiquitous Leaf Commensals Reveals Complementary Adaptive Traits for
835 Phyllosphere Colonization. *Mol Cell Proteomics* **15**(10): 3256-3269.

Müller DB, Vogel C, Bai Y, Vorholt JA. 2016b. The Plant Microbiota: Systems-Level Insights and Perspectives. *Annu Rev Genet* **50**: 211-234.

Murdoch CC, Skaar EP. 2022. Nutritional immunity: the battle for nutrient metals at the host-pathogen interface. *Nat Rev Microbiol* **20**(11): 657-670.

Nagakubo S, Nishino K, Hirata T, Yamaguchi A. 2002. The putative response regulator BaeR stimulates multidrug resistance of *Escherichia coli* via a novel multidrug exporter system, MdtABC. *J Bacteriol* **184**(15): 4161-4167.

Nathan C, Shiloh MU. 2000. Reactive oxygen and nitrogen intermediates in the relationship between mammalian hosts and microbial pathogens. *Proc Natl Acad Sci U S A* **97**(16): 8841-8848.

Nieboer E, and Richardson, D.H.S. 1980. The replacement of the nondescript term "heavy metals" by a biologically and chemically significant classification of metal ions. *Environ Poll Series B - Chem Phys 1, 3-26*.

Nies DH. 1992a. CzcR and CzcD, gene products affecting regulation of resistance to cobalt, zinc, and cadmium (czc system) in *Alcaligenes eutrophus*. *J Bacteriol* **174**(24): 8102-8110.

Nies DH. 1992b. Resistance to cadmium, cobalt, zinc, and nickel in microbes. *Plasmid* **27**(1): 17-28.

Nies DH, Grass G. 2009. Transition metal homeostasis. *EcoSal Plus* **3**(2): 10-1128.

Nies DH, Nies A, Chu L, Silver S. 1989. Expression and nucleotide sequence of a plasmid-determined divalent cation efflux system from *Alcaligenes eutrophus*. *Proc Natl Acad Sci USA* **86**(19): 7351-7355.

Nies DH, Silver S. 1989. Plasmid-determined inducible efflux is responsible for resistance to cadmium, zinc, and cobalt in *Alcaligenes eutrophus*. *J Bacteriol* **171**(2): 896-900.

Nieto JJ, Ventosa A, Ruiz-Berraquero F. 1987. Susceptibility of halobacteria to heavy metals. *Appl Environ Microbiol* **53**(5): 1199-1202.

Nishino K, Nikaido E, Yamaguchi A. 2007. Regulation of multidrug efflux systems involved in multidrug and metal resistance of *Salmonella enterica* serovar *typhimurium*. *J Bacteriol* **189**(24): 9066-9075.

Norvell WA 1991. Reactions of Metal Chelates in Soils and Nutrient Solutions. *Micronutrients in Agriculture*, 187-227.

O'Leary BM, Rico A, McCraw S, Fones HN, Preston GM. 2014. The infiltration-centrifugation technique for extraction of apoplastic fluid from plant leaves using *Phaseolus vulgaris* as an example. *J Vis Exp*(94): 52113.

Outten CE, Outten FW, O'Halloran TV. 1999. DNA distortion mechanism for transcriptional activation by ZntR, a Zn(II)-responsive MerR homologue in *Escherichia coli*. *J Biol Chem* **274**(53): 37517-37524.

Pais In, Jones JB. 1997. *The handbook of trace elements*. Boca Raton, Fla.: St. Lucie Press.

Pfeilmeier S, Petti GC, Bortfeld-Miller M, Daniel B, Field CM, Sunagawa S, Vorholt JA. 2021. The plant NADPH oxidase RBOHD is required for microbiota homeostasis in leaves. *Nat Microbiol* **6**(7): 852-864.

R_Core_Team 2020. R: A language and environment for statistical computing. Vienna, Austria: R Foundation for Statistical Computing.

Rensing C, Mitra B, Rosen BP. 1997. The *zntA* gene of *Escherichia coli* encodes a Zn(II)-translocating P-type ATPase. *Proc Natl Acad Sci USA* **94**(26): 14326-14331.

Ritpitakphong U, Falquet L, Vimoltust A, Berger A, Metraux JP, L'Haridon F. 2016. The microbiome of the leaf surface of Arabidopsis protects against a fungal pathogen. *New Phytol* **210**(3): 1033-1043.

Robb J, Lee SW, Mohan R, Kolattukudy PE. 1991. Chemical characterization of stress-induced vascular coating in tomato. *Plant Physiol* **97**(2): 528-536.

Robbins C, Thiergart T, Hacquard S, Garrido-Oter R, Gans W, Peiter E, Schulze-Lefert P, Spaepen S. 2018. Root-associated bacterial and fungal community profiles of *Arabidopsis thaliana* are robust across contrasting soil P levels. *Phytobiomes* **2**(1): 24-34.

RStudio_Team. 2021. RStudio: Integrated Development Environment for R. RStudio, PBC, Boston, MA, http://www.rstudio.com/.

Samanovic MI, Ding C, Thiele DJ, Darwin KH. 2012. Copper in microbial pathogenesis: meddling with the metal. *Cell Host Microbe* **11**(2): 106-115.

Sattelmacher B. 2001. The apoplast and its significance for plant mineral nutrition. *New Phytol* **149**(2): 167-192.

Silver S, Walderhaug M. 1992. Gene regulation of plasmid- and chromosome-determined inorganic ion transport in bacteria. *Microbiol Rev* **56**(1): 195-228.

Singh VK, Xiong A, Usgaard TR, Chakrabarti S, Deora R, Misra TK, Jayaswal RK. 1999. ZntR is an autoregulatory protein and negatively regulates the chromosomal zinc resistance operon *znt* of *Staphylococcus aureus*. *Mol Microbiol* **33**(1): 200-207.

Stein RJ, Höreth S, de Melo JR, Syllwasschy L, Lee G, Garbin ML, Clemens S, Krämer U. 2017. Relationships between soil and leaf mineral composition are element-specific, environment-dependent and geographically structured in the emerging model *Arabidopsis halleri*. *New Phytol* **213**(3): 1274-1286.

Sterckeman T, Thomine S. 2020. Mechanisms of Cadmium Accumulation in Plants. *Crit Rev Plant Sci* **39**(4): 322-359.

Tada Y, Inoue T. 2000. Use of oligotrophic bacteria for the biological monitoring of heavy metals. *J Appl Microbiol* **88**(1): 154-160.

Torres MA, Dangl JL, Jones JDG. 2002. Arabidopsis gp91phox homologues AtrbohD and AtrbohF are required for accumulation of reactive oxygen intermediates in the plant defense response. *Proc Natl Acad Sci USA* **99**(1): 517-522.

Vert G, Grotz N, Dedaldechamp F, Gaymard F, Guerinot ML, Briat JF, Curie C. 2002. IRT1, an Arabidopsis transporter essential for iron uptake from the soil and for plant growth. *Plant Cell* **14**(6): 1223-1233.

Vogel C, Bodenhausen N, Gruissem W, Vorholt JA. 2016. The Arabidopsis leaf transcriptome reveals distinct but also overlapping responses to colonization by phyllosphere commensals and pathogen infection with impact on plant health. *New Phytol* **212**(1): 192-207.

Vogel CM, Potthoff DB, Schafer M, Barandun N, Vorholt JA. 2021. Protective role of the Arabidopsis leaf microbiota against a bacterial pathogen. *Nat Microbiol* **6**(12): 1537-1548.

Vorholt JA. 2012. Microbial life in the phyllosphere. *Nat Rev Microbiol* **10**(12): 828-840.

White C, Lee J, Kambe T, Fritsche K, Petris MJ. 2009. A role for the ATP7A copper-transporting ATPase in macrophage bactericidal activity. *J Biol Chem* **284**(49): 33949-33956.

Williams B. 2007. The chemistry of evolution: the development of our ecosystem. *Choice: Curr Rev Acad Libr* **44**(7): 1197-1197.

927 **Xia H, Yu Y, Chen Z, Liu H, Wang T, Huang W, Chu Z. 2026.** COPT4 interacts with COPT1
928 or COPT3 to manipulate the signaling response for copper-triggered immunity in
929 Arabidopsis. *New Phytol* **in press**.
930 **Yang H-C, Rosen BP. 2016.** New mechanisms of bacterial arsenic resistance. *Biomed J* **39**(1): 5-
931 13.
932 **Zhao C, Zhang Y, Chan Z, Chen S, Yang S. 2015.** Insights into arsenic multi-operons
933 expression and resistance mechanisms in *Rhodopseudomonas palustris* CGA009. *Front*
934 *Microbiol* **6**: 986.

935 ## Supporting Information

936 **Dataset S1.** Maximum permissive metal concentrations.
937 **Dataset S2.** KEGG orthologous gene groups and genes of interest (GoI).
938 **Dataset S3.** Genomic presence/absence of genes based on Kegg Orthologue (KO) identifiers.
939 **Dataset S4.** Effects of previously described metal-related genes on tolerance levels (median
940 MPC) in At-LSPHERE strains.
941 **Dataset S5.** Elemental concentrations and glucose-6-phosphate dehydrogenase (G6PDH)
942 activity in AWF in a set-up experiment.
943 **Dataset S6.** Loadings of genes on principal components (Figure 6A).
944 **Dataset S7.** Genomic presence/absence and copy numbers of Cd-related genes and gene scores
945 (Figure 6B).

946 **Figure S1.** Taxonomic structure of synthetic communities.
947 **Figure S2.** Cd tolerance of synthetic bacterial communities and single strains on agar-solidified
948 R2A media.
949 **Figure S3.** Cd tolerance of synthetic bacterial communities based on growth curves in liquid
950 R2A media.
951 **Figure S4.** Ionomes of leaf and leaf apoplast samples of *A. thaliana*.
952 **Figure S5.** Cd tolerance of keystone strains in liquid media.
953 **Figure S6.** Relationship between metal tolerance profiles and phylogeny of *At*-LSPHERE
954 strains.
955 **Figure S7.** Relationship between metal-related genes in the genome and phylogeny of *At*-
956 LSPHERE strains.

957 **Table S1.** Composition of R2A medium.
958 **Table S2.** Metal salts used in tolerance screening on solid R2A medium.
959 **Table S3.** Total concentrations of elements in R2A media as quantified by ICP-OES.
960 **Table S4.** Cd tolerances of individual strains of the synthetic communities.
961 **Table S5.** The ionome of the *A. thaliana* leaf apoplastic fluid.
962 **Table S6.** Soil ionomes for the greenhouse soil and the field-collected soil mixtures used for
963 plant cultivation.

964 **Table S7.** Leaf ionomes before and after AWF extraction for *A. thaliana* grown in greenhouse
965 soil or field soil mixture.
966 **Table S8.** Combined effects of cadmium and copper toxicity on keystone strains.
967 **Table S9.** Combined effects of cadmium, zinc and manganese on keystone strains.
968 **Table S10.** Known metal-related genes associated with metal tolerances in the *At*-LSPHERE
969 collection.

970 **Supporting Information - Supplementary Methods Text**

Table 1. Effective concentrations of metals for the Arabidopsis phyllosphere (*At*-LSPHERE) and associated soil bacterial strain collections. (based on curve fits).

***At*-LSPHERE bacterial strain collection**				
Element	**EC_5 [mM][a]**	**EC_{50} [mM][a]**	**EC_{95} [mM][a]**	**Concentration range[c]**
Cd^{II}	4.3×10^{-3}	0.049	0.56	130
Cu^{II}	0.11	0.42	1.6	15
Zn^{II}	0.046	0.50	5.6	120
As^{III}	0.17	1.1	6.6	40
Mn^{II}	1.9	9.2	46	25
As^{V}	~0.32[b]	147[b]	> 150[b]	>> 100[b]
Soil bacterial strain collection				
Element	**EC_5 [mM][a]**	**EC_{50} [mM][a]**	**EC_{95} [mM][a]**	**Concentration range[c]**
Cd^{II}	2.0×10^{-3}	0.010	0.054	27
Cu^{II}	0.25	0.60	1.4	5.6
Zn^{II}	0.040	0.16	0.66	17
As^{III}	0.087	1.1	14	160
Mn^{II}	0.77	15	> 100[b]	>> 100[b]
As^{V}	~0.40[b]	27[b]	> 100[b]	>> 100[b]

[a]EC_n denote metal concentration preventing growth of *n*% of the tested bacterial strains, based on curve fits (see Fig. 1a and b, Dataset S1, and Methods).

[b]Values estimated from experiments (no curve fit possible).

[c]Defined here as EC_{95}:EC_5 ratio.

971

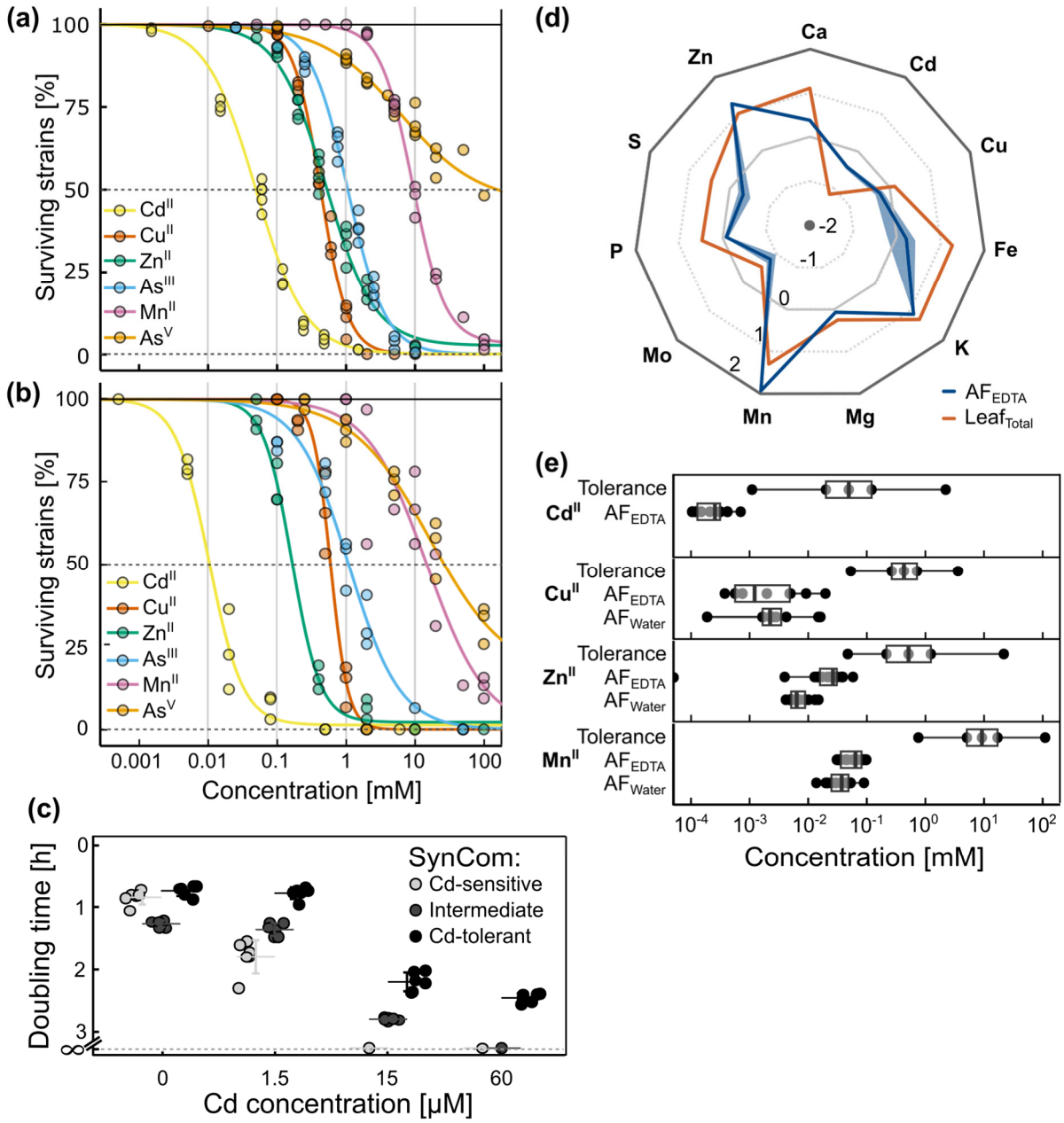

Figure 1. Metal(loid) tolerances of phyllosphere bacterial strains in relation to the leaf apoplastic fluid ionome of *A. thaliana*. (a, b) Metal(loid) dose-response curves for the phyllosphere bacterial collection (a, *At*-LSPHERE, n = 224 strains) and for a bacterial strain collection from unplanted soils (b, n = 33) (Bai et al. 2015). Each strain was spotted on agar-solidified R2A medium supplemented with a series of metal(loid) concentrations. Replicate data points represent independent experiments; lines are curve fits (see Methods, Dataset S1). **(c)** Cd tolerance of synthetic bacterial communities (SynComs; datapoints shown by circles, bars mark mean ± SD, n = 6 technical replicates; data from one experiment representative of a total of four independent experiments). Apparent doubling times of the SynComs were calculated based on the earliest identifiable log phase of growth from time series of OD_{600} measurements with cultivation at 26°C for 24 h (see Fig. S3). ∞: no growth. Note that the horizontal axis is not scaled. **(d)** Ionome of leaf apoplastic fluid (AF_{EDTA}, blue line), and of the entire fresh leaf ($Leaf_{Total}$, red line). Shown is the average (line) and the standard deviation (shadow) for each element as Log_{10} of the concentration ([mM] for Ca, S, P, Mg, and K; [µM] for Zn, Mo, Mn, Fe, Cu, and Cd; n = 4 samples for AF and n = 3 samples for leaves). **(e)** Boxplots showing metal concentrations in apoplastic fluid (AF_{EDTA}, AF_{Water}: extracted in 100

µM EDTA and in water, respectively) of soil-grown plants, alongside metal tolerance of the *At*-LSPHERE collection (re-plotted from (a)). For AF, boxes show median (central line), 25%/75%ile (box), and maximum/minimum (bars) of all measurements (n = 17; see Table S5, Fig. S4e-g). For metal tolerances, boxes show effective concentration EC_{50} (central line), EC_{25}/EC_{75} (boxes) and EC_{1}/EC_{99} (bars)(see Table 1, and Materials and Methods). Dose-response curves are from a minimum of 3 independent experiments conducted on R2A medium (a, b). AF data are from one representative experiment (d; Table S5, GHs 4; Fig. S4e-g, E4) and from 4 independent experiments conducted on greenhouse soil (e). Not shown: AF_{Water} for Cd and data for As were below our detection limits (d, e).

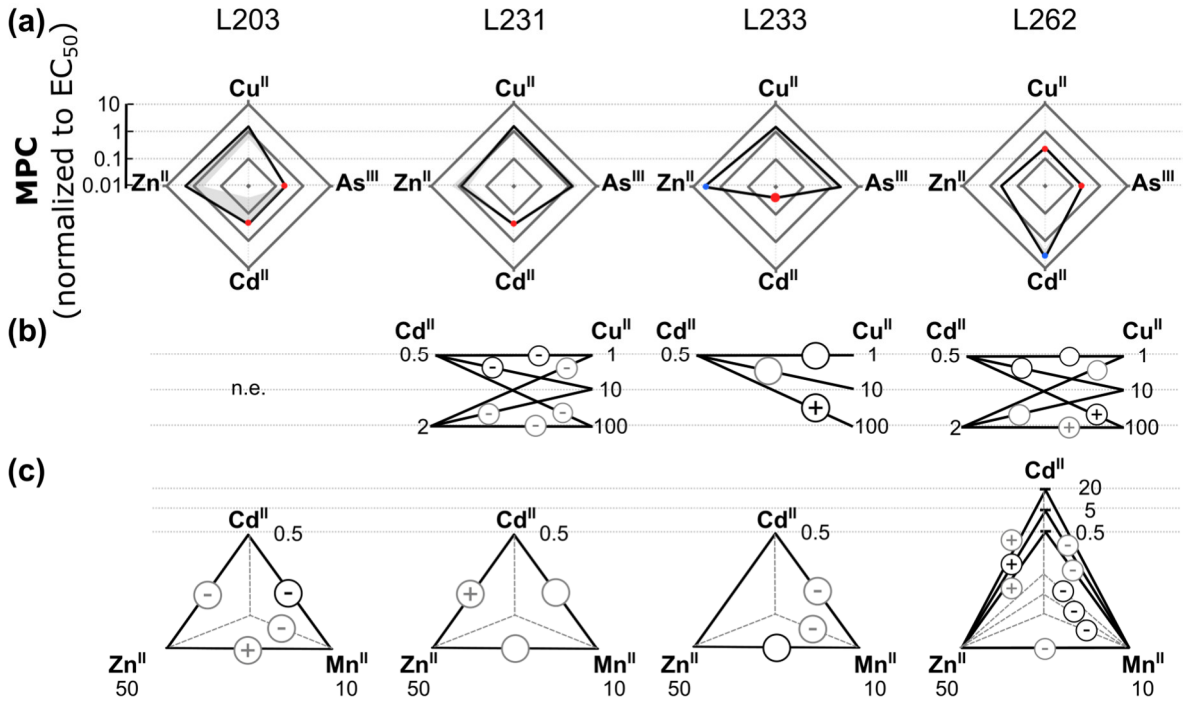

Figure 2. Metal(loid) tolerance profiles of keystone strains of the *A. thaliana* phyllosphere bacterial community. **(a)** Profiles of maximum permissive concentrations (MPC) normalized to EC_{50} on solid R2A media. Shown are median values (connected by black lines), with minima and maxima (grey shadows, n = 3 independent experiments), on a Log_{10} scale (1 reflects an MPC equivalent to EC_{50}, see Table 1, Dataset S1). Values below 0.5 (small red)/0.05 (large red) and above 5 (small blue) are shown as colored circular shapes. Mn is not shown because of its low toxicity in these strains. **(b, c)** Combined toxicity effects of Cd and Cu (b), and Cd, Zn, and Mn (c) on keystone strains in liquid R2A media (see Tables S8 and S9). Symbols show combined toxicity-enhancing (+) and toxicity-alleviating (-) effects of the metals connected by the corresponding black line; numbers are concentrations [µM]. Results reproduced in three/two out of three independent experiments are shown in black/grey color. Grey dotted lines: effect of the adjacent metal on the combined toxicity of the other two metals (c). Data not shown (n.e.: results could not be evaluated because of metal sensitivity, b). Circle sizes adjusted to fit.

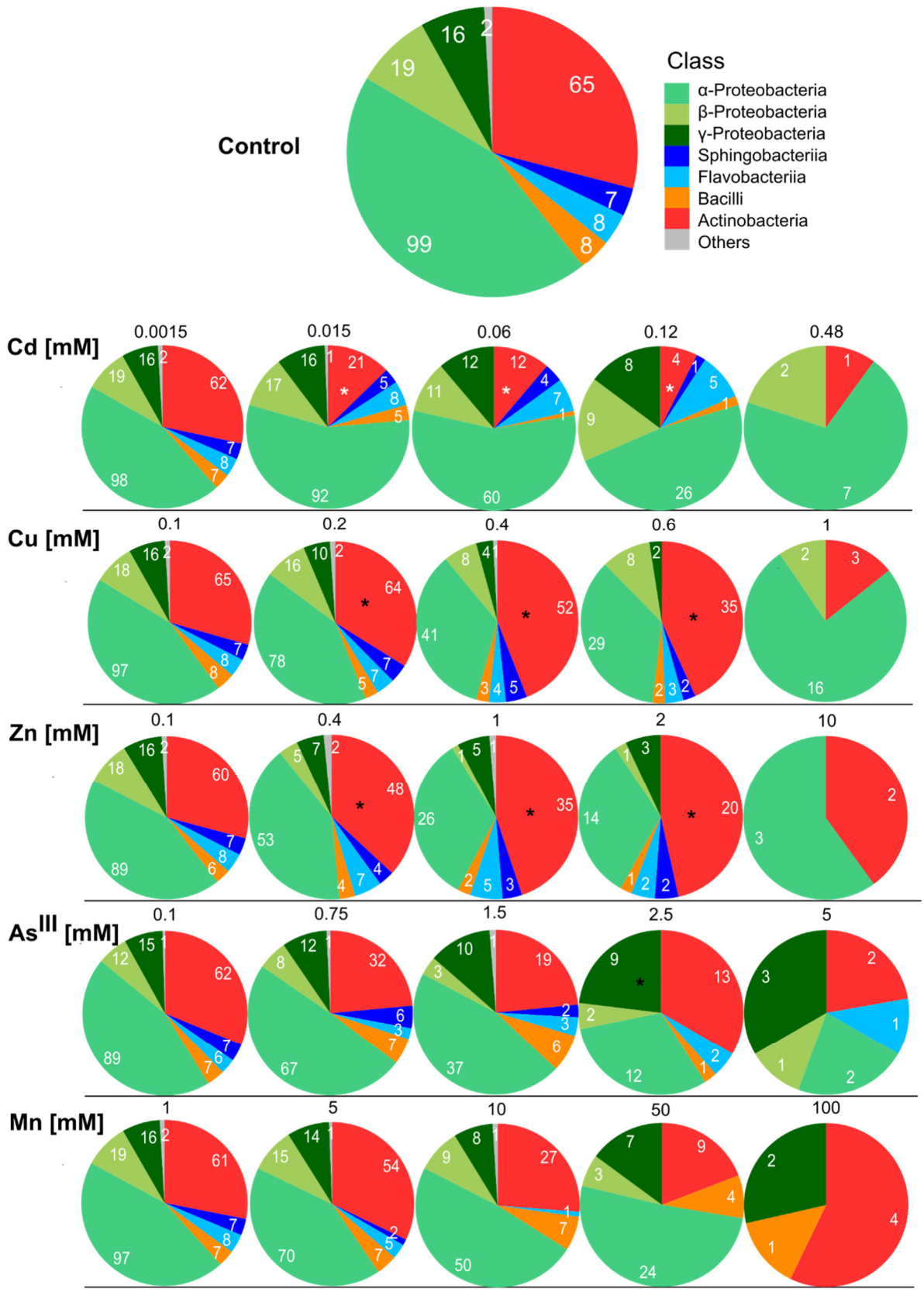

Figure 3. Effects of metal(loid) tolerances of *At*-LSPHERE bacterial strains on the phylogenetic structure among the survivors. Pie fractions reflect the percentage share (with the number given in white) out of all bacterial strains that were able to grow under a given condition (Dataset S1). The metal(loid) concentration is given in black fonts above the chart for each treatment. Asterisks mark significant enrichment (*, black) or depletion (*, white) compared to the control condition (Fisher's exact test, *q-value* < 0.05).

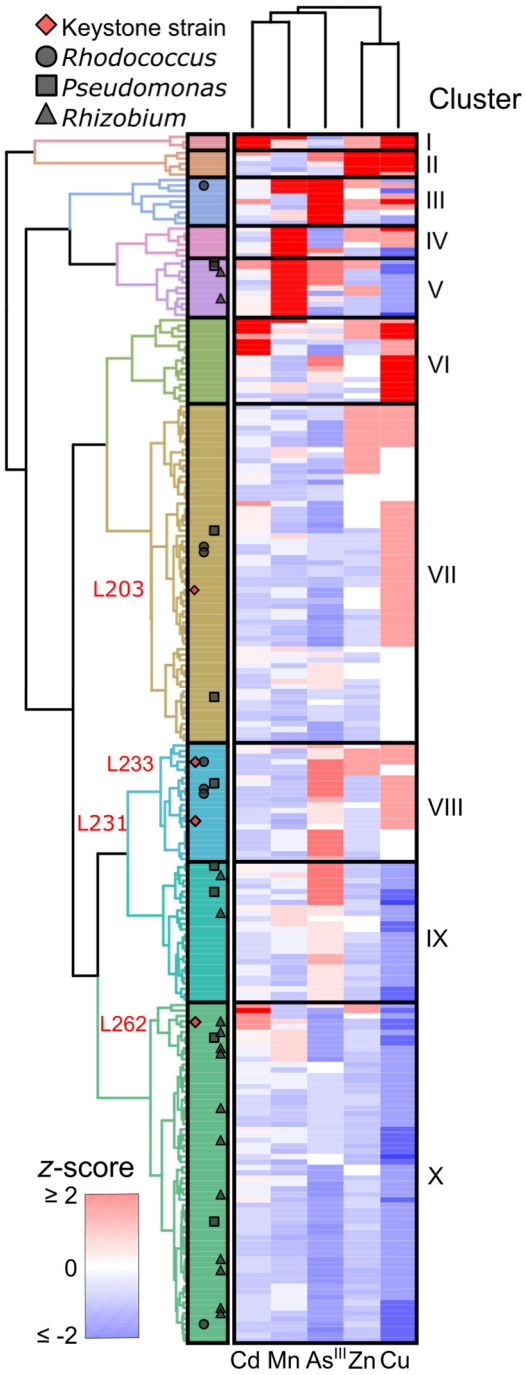

Figure 4. Hierarchical clustering of strains according to their metal(loid) tolerance profiles. Maximum permissive concentrations of Cd, Zn, Cu, arsenite, and Mn in the *At*-LSPHERE strains (Dataset S1) were clustered by Euclidean distance-based (Ward) clustering (*z*-score-based). Clusters (I to X) are emphasized by different colors (left) and separated by horizontal lines. Symbols mark the positions of *Rhodococcus (n* = 6), *Pseudomonas* (*n* = 9), *Rhizobium* (*n* = 15), and keystone strains (*n* = 4).

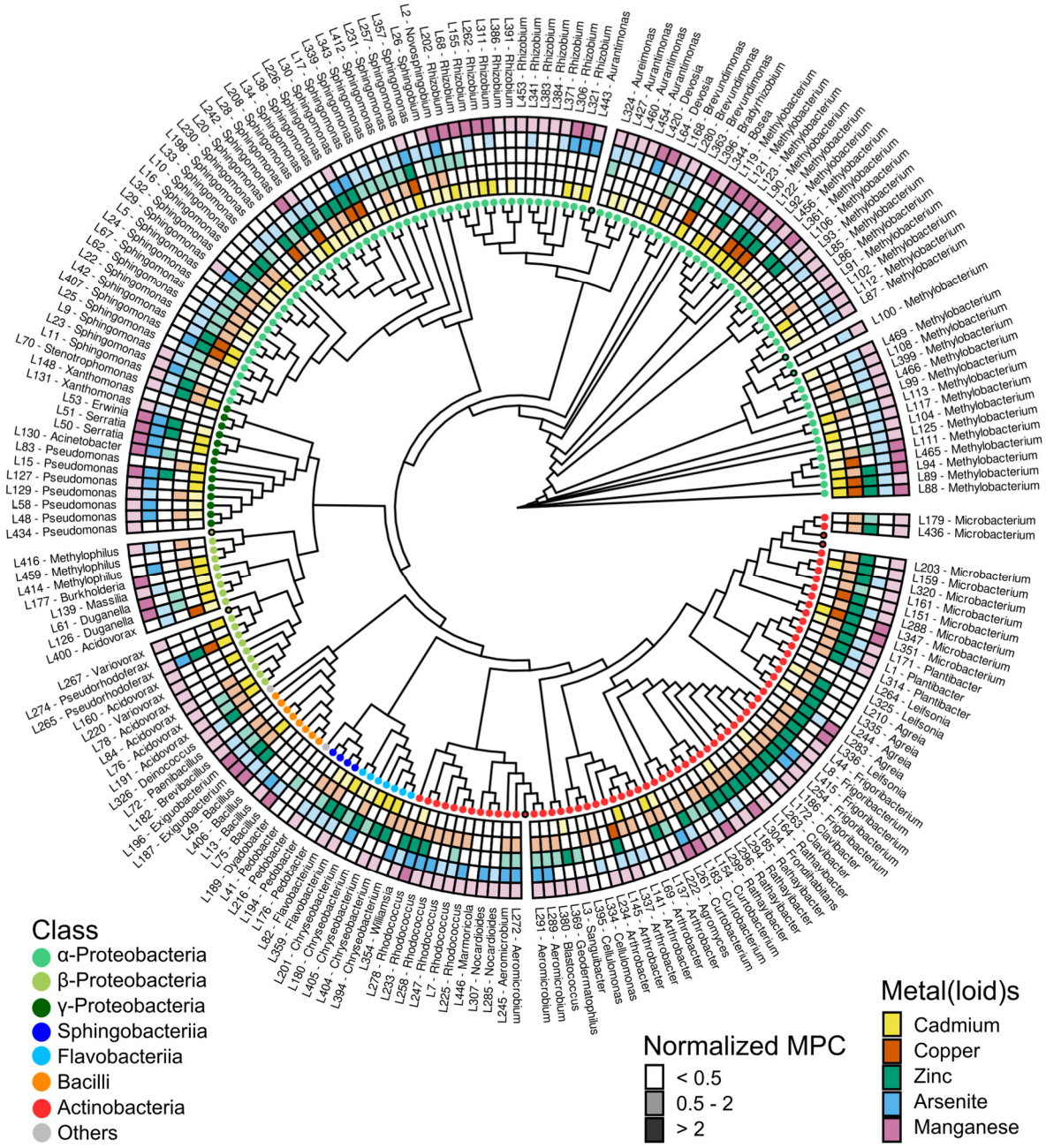

Figure 5. Strain-specific metal(loid) tolerances shown over the phylogeny of the *At*-LSPHERE strain collection. Cladogram of the *At*-LSPHERE strain collection (n = 214; 16s rRNA-based (Bai et al. 2015)) with circular heatmap representations of relative tolerance. Heatmap color shade reflects strain-wise maximum permissive concentrations (MPC, median of n = 3 independent experiments; Dataset S1) normalized to the EC_{50}, the concentration eliminating the growth of 50% of all bacterial strains (Cd: 0.049 mM, Zn: 0.5 mM, Cu: 0.4 mM, As^{III}: 1.1 mM, Mn: 9.2 mM; Table 1). Strains (n = 8) not profiled for metal tolerance are marked by a black line around the colored circle.

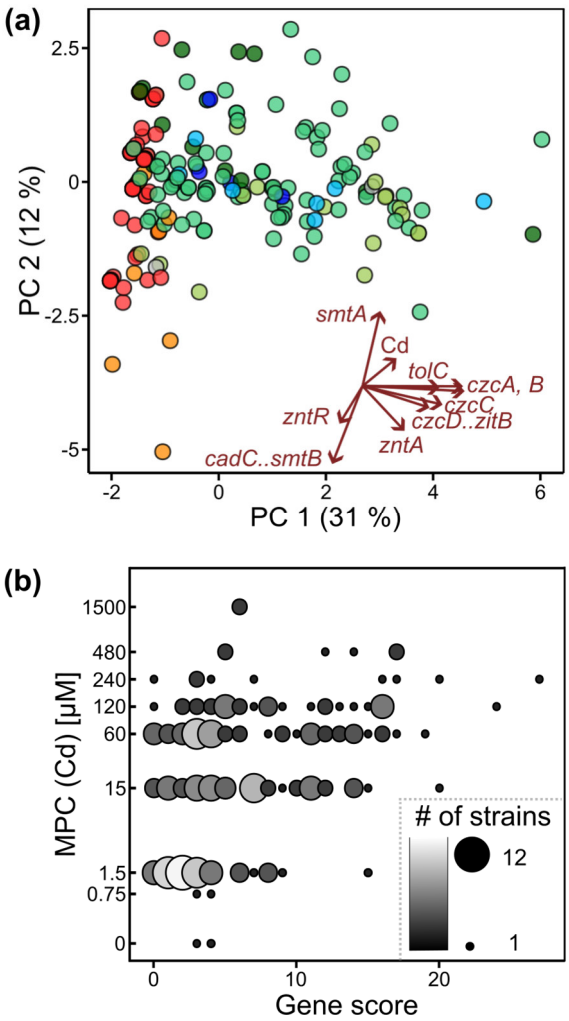

Figure 6. Relationships between known Cd tolerance genes and Cd tolerance of *At*-LSPHERE strains. (a) PCA of strain-wise maximum permissive Cd concentrations (MPC, *z*-score-based) and presence/absence of known Cd tolerance-related genes. Each datapoint represents one strain (Datasets S1-S3). The percentages of variation accounted for by each significant PC are given in parentheses (95% confidence intervals: PC 1, 31% to 36.7%; PC 2, 10.9% to 13.8%; bootstrapping with 999 replicates). KEGG Orthology (KO) identifiers with significant loadings on PC1 are: *czcA–D* and *tolC* (alternative short names linked by "..."; Dataset S6). **(b)** Plot of strain-wise maximum permissive Cd concentration (MPC, absolute) against a gene score incorporating both presence/absence and copy number of known Cd tolerance-related genes. Each datapoint represents one strain (Datasets S1-S3). The gene score of a strain is the genome-wide sum of genes and gene copies with previously published roles in Cd tolerance (Kendall's rank correlation, $\tau = 0.31$, $p = 3.5\times10^{-9}$; Dataset S7).

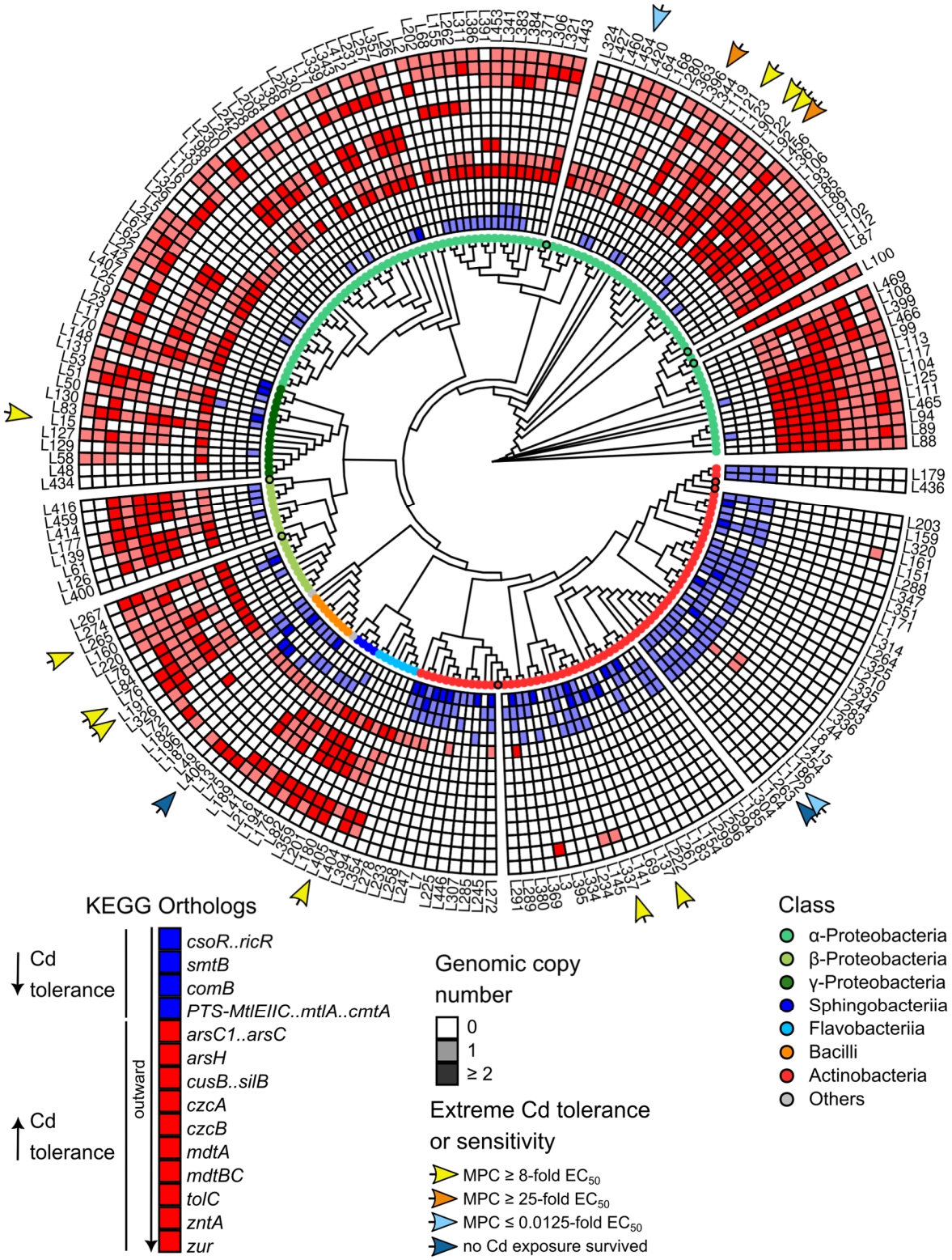

Figure 7. Metal(loid)-related genes implicated in Cd tolerance of *At*-LSPHERE strains shown over phylogeny. Shown are known metal(loid)-related genes of which the presence in the genome was statistically associated with altered Cd tolerance in our study ($p_{adj} < 0.005$, for *arsH* $p_{adj} = 0.023$; with Bonferroni corrections). Colors of KO identifiers reflect whether the median of maximum permissive concentrations (MPC median) of all positive strains was > 2-fold higher (red) or > 2-fold lower (blue) than that of all strains lacking an orthologue (Dataset S4; else KO id. not shown). Genes (KO identifiers) are only shown if present in at least 30 bacterial strains (Dataset S4). Strains ($n = 8$) not profiled for metal tolerance are marked by a black line around the colored circle.